AD-A051 197 VIRGINIA POLYTECHNIC INST AND STATE UNIV BLACKSBURG --ETC F/G 20/4
THREE-DIMENSIONAL INCOMPRESSIBLE BOUNDARY LAYERS ON BLUNT BODIE--ETC(U)
MAY 77 D L DWOYER, C H LEWIS, P R GOGINENI

UNCLASSIFIED VPI/SU-AERO-063 NL

1 OF 1
ADA
051197

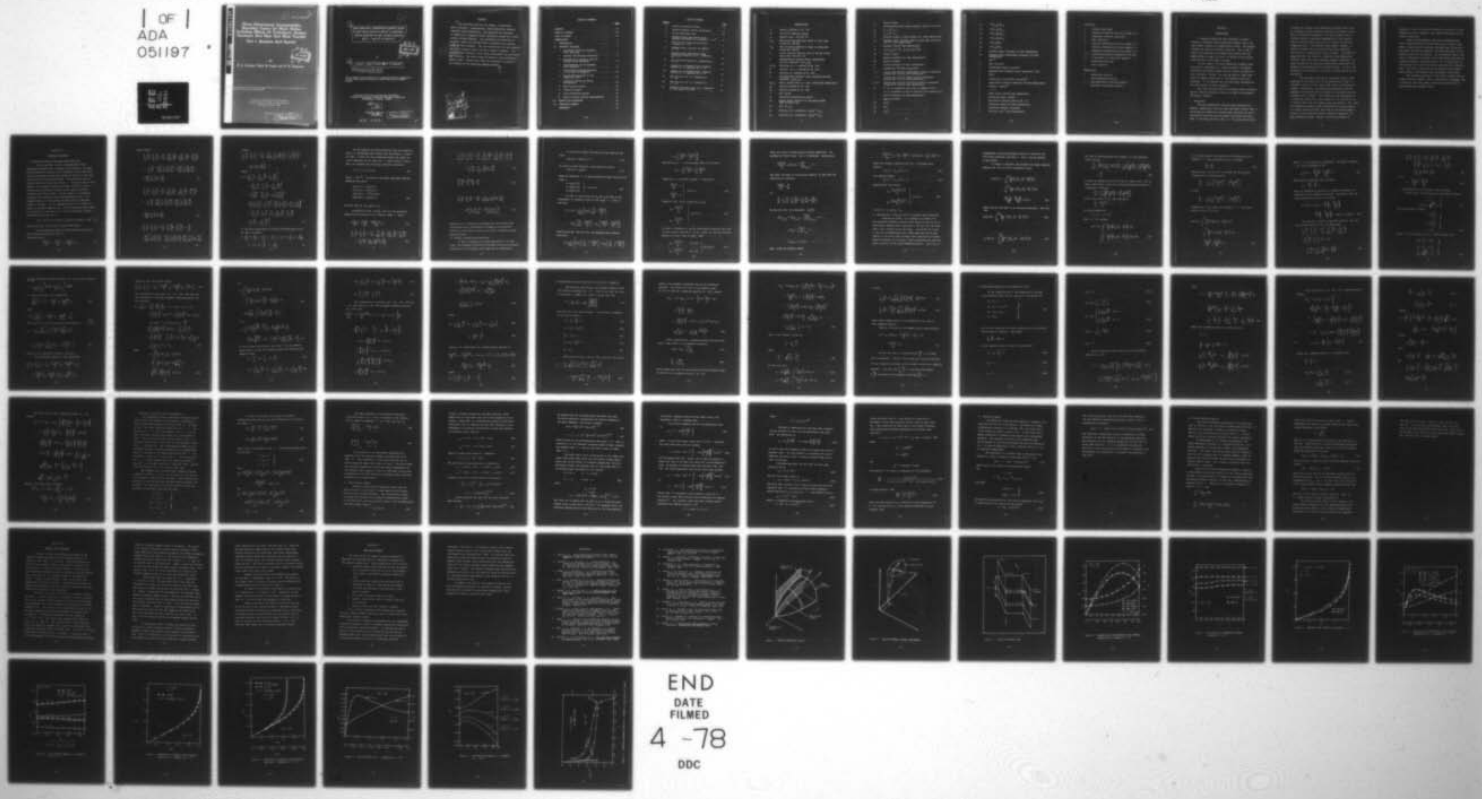

END
DATE
FILMED
4 -78
DDC

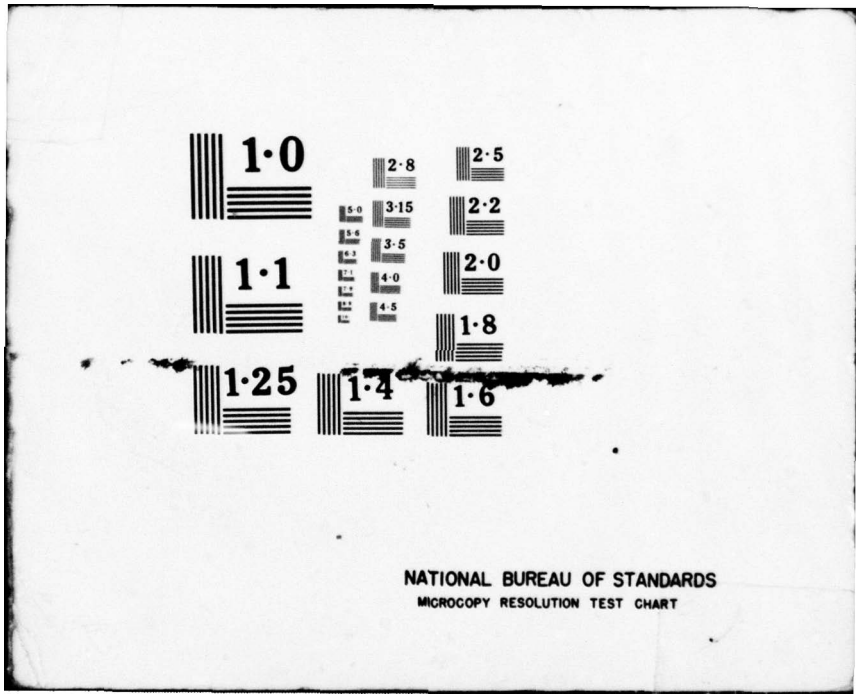
1·0
1·1
1·25
1·4
1·6
1·8
2·0
2·2
2·5
2·8
3·15
3·5
4·0
4·5
5·0
NATIONAL BUREAU OF STANDARDS
MICROCOPY RESOLUTION TEST CHART

VPI & SU AERO-063

Three-Dimensional Incompressible Boundary Layers On Blunt Bodies Including Effects Of Turbulence, Surface Curvature And Heat And Mass Transfer

Part 1: Analysis And Results

by

D. L. Dwoyer, Clark H. Lewis and P. R. Gogineni

This research was sponsored by the Applied Physics Laboratory of the Johns Hopkins University under Subcontract Number 600325.

Aerospace and Ocean Engineering Department
Virginia Polytechnic Institute and State University
Blacksburg, Virginia 24061

May 1977

(1)

(6)

THREE-DIMENSIONAL INCOMPRESSIBLE BOUNDARY LAYERS ON BLUNT BODIES INCLUDING EFFECTS OF TURBULENCE, SURFACE CURVATURE AND HEAT AND MASS TRANSFER. PART 1. ANALYSIS AND RESULTS,

by

(10) D. L./Dwoyer, Clark H./Lewis [redacted] P. R./Gogineni

(14) VPI/SU-AERO-063

This research was sponsored by the Applied Physics Laboratory of the Johns Hopkins University under Subcontract Number 600325.

Aerospace and Ocean Engineering Department
Virginia Polytechnic Institute and State University
Blacksburg, Virginia 24061

(12) 74p.

(11) May [redacted]77

406 922

IV

ABSTRACT

The governing equations for laminar, transitional and/or turbulent, incompressible, three-dimensional boundary layers are solved numerically. The equations are developed in terms of an orthogonal surface coordinate system and include surface curvature effects. The coordinates are generated numerically, while the inviscid flow is obtained from a general potential flow procedure. The only restrictions on body geometry are that it possess a blunt nose and a plane of symmetry. The boundary-layer equations, after being transformed into similarity type variables, are solved using the implicit finite-difference Krause scheme. Various test cases are presented to establish the accuracy of the resulting computer program.

TABLE OF CONTENTS

LIST OF FIGURES

NOMENCLATURE

A	Quantity defined in Eq. (47)
A^*	Van Driest damping constant
C	Specific heat, $ft^2/sec^2\text{-}^oR$
C_{f_e}	Skin friction coefficient based on local edge properties $\tau/\frac{1}{2}\rho U_e^2$
C_{f_∞}	Skin friction coefficient based on freestream properties $\tau/\frac{1}{2}\rho U_\infty^2$
E	Scalar velocity function used in the Van Driest inner eddy viscosity law
F	Nondimensional boundary-layer longitudinal velocity component $h_\xi U/h_{\xi,0}U_e$
F_1, F_2	Functions of ξ, ω defined by Eq. (20)
$\bar{F}$	Function of ξ, ω defined by Eq. (25)
$\tilde{F}$	Function of ξ defined by Eq. (29)
G	Nondimensional boundary layer crossflow velocity component, $h_\omega w/h_{\omega,0}W$
h_ξ, h_ω	Metric coefficients in ξ and ω directions respectively
H_m	Quantity defined by Eq. (51)
H_θ	Quantity defined by Eq. (56)
i	Unit vector
I_f	Transition intermittancy factor
k_*	Mixing length constant for Van Driest inner eddy viscosity law
k_ξ	$h_{\xi,0}^{-1}\,(h_{\xi,n})_0$
K_ξ	Curvature of ξ coordinate, $(h_\xi h_\omega)^{-1}\,h_{\xi,\omega}$
K_ω	Curvature of ω coordinate, $(h_\xi h_\omega)^{-1}\,h_{\omega,\xi}$

ℓ_*	Mixing length
L	Nondimensionalizing length normally taken as one foot
L_ξ	$h_{\xi,0}\, h_\xi^{-3}\, h_{\xi,\xi}$
L_ω	$h_{\omega,0}\, h_\omega^{-3}\, h_{\omega,\omega}$
n	Distance normal to body surface (ft when dimensional)
n_ℓ	Boundary layer thickness used in outer eddy viscosity law (ft. when dimensional)
p	Pressure (lb/ft^2 when dimensional)
Q	$-\frac{1}{2}\,(h_{\xi,0}/h_\xi)^2\, U_e^2 - \frac{1}{2}\,(h_{\omega,0}/h_\omega)^2\, W_e^2$
Pr	Prandtl number
r	Radial coordinate (ft when dimensional)
Re	Reynolds number
S	Surface distance (ft when dimensional)
T	Temperature (^oR when dimensional)
u, U	Viscous and inviscid longitudinal velocity components respectively (ft/sec when dimensional)
v, V	Viscous and inviscid normal velocity components respectively (ft/sec when dimensional)
w, W	Viscous and inviscid cross-flow velocity components respectively (ft/sec when dimensional)
W	$W = W_e$ at stagnation point and in symmetry plane, $W = U_e$ elsewhere as used in Sections II-4 through II-6
x	Axial coordinate (ft when dimensional)
α	Angle of attack
$\bar{\alpha}_1$	W_e/U_e
$\bar{\alpha}_2$	W/U_e
$\bar{\alpha}_3$	W_e/W

β_1	$(\xi/h_{\xi,0}U_e)U_{e,\xi}$
β_2	$(\xi/h_{\omega,0}U_e)U_{e,\omega}$
β_3	$(\xi/h_{\xi,0}W_e)W_{e,\xi}$
β_4	$(\xi/h_{\omega,0}W_e)W_{e,\omega}$
β_5	$(\xi/h_{\xi,0}W)W_{\xi}$
β_6	$(\xi/h_{\omega,0}W)W_{\omega}$
δ	Boundary-layer thickness (ft when dimensional)
δ^*	Boundary-layer displacement thickness (ft when dimensional)
ε	$Re^{-1/2}$
ε^+	Eddy viscosity
η	Transformed normal coordinate
θ	Nondimensional boundary-layer temperature, T/T_e
λ	U_e^2/T_e
μ	Coefficient of viscosity, lb-sec/ft^2
ξ	Longitudinal surface coordinate (ft when dimensional)
ρ	Density, slugs/ft^3
σ	$1 + \varepsilon^+$
τ	Shear stress (lb/ft^2 when dimensional)
ϕ	Meridional angle, degrees
Φ	Dissipation function given by Eq. (7)
$\overline{\chi}$	Transition length (ft when dimensional)
ω	Transverse surface coordinate
Ω	Vorticity (sec^{-1} when dimensional)

Subscripts

e	Boundary-layer edge
n	Indicates differentiation with respect to n
t	Designates turbulent quantities
0	Wall conditions
η	Indicates differentiation with respect to η
ξ	Indicates differentiation with respect to ξ
ω	Indicates differentiation with respect to ω
$\xi,0$	ξ-direction quantity evaluated at the wall
ξ,ξ	ξ derivative of ξ-direction quantity
∞	Freestream conditions
$\underline{\quad}$	Vector quantity

Superscripts

*	Dimensional quantity
~	Non-dimensional quantity
$\overline{\quad}$	Non-dimensional stretched quantity
'	Turbulent fluctuating quantity

SECTION I

INTRODUCTION

A computer program has been developed to predict laminar or turbulent three-dimensional boundary layers over blunt bodies immersed in incompressible fluids. The program includes the effects of surface curvature. Such a code is useful for predicting the boundary-layer growth over submerged bodies at angle of attack, or bodies of non-circular cross-section at zero angle of attack.

In this report, the three-dimensional boundary-layer equations are developed in a surface-oriented, orthogonal, curvilinear coordinate system with all surface curvature effects included. Further, the limiting forms of these equations in symmetry planes and at the stagnation point are developed. It is required that any body shape considered by the code possess a plane of symmetry.

The resulting equations are integrated using a marching, implicit finite-difference scheme on an IBM 370 system-model 158 digital computer.

1. Background

The three-dimensional boundary-layer equations for laminar, compressible flow have been developed by Moore (Ref. 1). Procedures for numerically solving these equations for the incompressible case have been developed by Blottner and Ellis (Ref. 2) and Chang and Patel (Ref. 3). The Blottner and Ellis

procedure for laminar three-dimensional boundary layers uses an orthogonal, surface-oriented, curvilinear coordinate system which is numerically generated. In this procedure, the coordinate system is developed independently of the boundary-layer or inviscid flow, but has as its origin the inviscid stagnation point. The procedure does require, however, an analytic solution for the inviscid flow and is therefore restricted to a rather narrow class of bodies. The method of Chang and Patel for laminar or turbulent three-dimensional boundary layers also uses orthogonal surface coordinates, but these coordinates are calculated analytically based upon the geometry of mathematically well defined shapes. As such, this procedure is also limited in the class of bodies which can be calculated.

The procedure developed in the present report takes advantage of the versatility of the Blottner-Ellis (Ref. 2) coordinate system so that a much wider class of bodies may be studied. Essentially, the numerically generated coordinate package of the Blottner-Ellis procedure is separated from the boundary-layer procedure. This allows for the development of a coordinate system for a given geometry to be carried out as a separate task from the boundary-layer calculation. Thus, once the coordinate system has been developed for a given geometry at a given angle of attack, that body can be studied under a variety of flow conditions without having to regenerate the body coordinate system. Further, since the procedure is

numerical, it can be used with a discrete description of body geometry as well as analytic, thus further enhancing the procedures versatility.

Since the body geometry that can be handled by the code is restricted only to blunt shapes with a plane of symmetry, a rather general technique for predicting the inviscid flow about the body is required. The Smith-Hess (Ref. 4) procedure is used for this purpose. An intermediate code is then used to interpolate the output of the Smith-Hess code onto the surface-orthogonal coordinate system. All of these data are then Fourier fitted and the Fourier coefficients are stored on disk. This disk is then read by the boundary-layer program which predicts the boundary-layer development on the body.

The technique described in this report accounts for all surface curvature effects, and, to the authors' knowledge, this is the first time these effects have been accounted for in three-dimensional boundary layers.

SECTION II

GOVERNING EQUATIONS

1. Coordinate System and Boundary-Layer Equations

In this section, the full incompressible three-dimensional boundary-layer equations are developed. The equations developed are written in an orthogonal curvilinear body-oriented coordinate system whose origin is located at the stagnation point for blunt nosed bodies. The details of the coordinate system are depicted in Fig. 1 . As can be seen in this figure, two coordinate systems are shown; the first a body-oriented polar coordinate system and the second a surface-oriented curvilinear system. In this system, ξ^* is measured away from the stagnation point along meridional cuts, ω^* is measured normal to ξ^* and around the body and n^* is measured normal to the body. At the stagnation point $\xi^* = 0$, and $\omega^* = 0$ along the windward symmetry cut. In this system the body radius r^* is generally a function of ω^*. For this coordinate system a differential distance ds^* is

$$ds^{*2} = h_{\xi}^{*2}\,(\xi^*,\omega^*,n^*)d\xi^{*2} + h_{\omega}^{*2}(\xi^*,\omega^*,n^*)d\omega^{*2} + dn^{*2} \qquad (1)$$

where h_{ξ}^* and h_{ω}^* are the metric scale coefficients.

The governing equations of fluid mechanics written in this coordinate system are (Ref. 5):

Incompressibility:

$$\frac{\partial(\tilde{h}_{\omega}\tilde{u})}{\partial\tilde{\xi}} + \frac{\partial(\tilde{h}_{\xi}\tilde{w})}{\partial\tilde{\omega}} + \frac{\partial(\tilde{h}_{\xi}\tilde{h}_{\omega}\tilde{v})}{\partial\tilde{n}} = 0 \qquad (2)$$

Navier Stokes

$$\frac{\tilde{u}}{\tilde{h}_\xi}\frac{\partial\tilde{u}}{\partial\tilde{\xi}} + \frac{\tilde{w}}{\tilde{h}_\omega}\frac{\partial\tilde{u}}{\partial\tilde{\omega}} + \tilde{v}\frac{\partial\tilde{u}}{\partial\tilde{n}} - \frac{\tilde{w}^2}{\tilde{h}_\xi\tilde{h}_\omega}\frac{\partial\tilde{h}_\omega}{\partial\tilde{\xi}} + \frac{\tilde{u}\tilde{w}}{\tilde{h}_\xi\tilde{h}_\omega}\frac{\partial\tilde{h}_\xi}{\partial\tilde{\omega}} + \frac{\tilde{u}\tilde{v}}{\tilde{h}_\xi}\frac{\partial\tilde{h}_\xi}{\partial\tilde{n}}$$

$$= -\frac{1}{\tilde{h}_\xi}\frac{\partial\tilde{p}}{\partial\tilde{\xi}} + \frac{Re^{-1}}{\tilde{h}_\xi\tilde{h}_\omega}\frac{\partial}{\partial\tilde{\xi}}\left(\frac{\tilde{h}_\omega}{\tilde{h}_\xi}\frac{\partial\tilde{u}}{\partial\tilde{\xi}}\right) + \frac{Re^{-1}}{\tilde{h}_\xi\tilde{h}_\omega}\frac{\partial}{\partial\tilde{\omega}}\left(\frac{\tilde{h}_\xi}{\tilde{h}_\omega}\frac{\partial\tilde{u}}{\partial\tilde{\omega}}\right)$$

$$+ \frac{Re^{-1}}{\tilde{h}_\xi\tilde{h}_\omega}\frac{\partial}{\partial\tilde{n}}\left(\tilde{h}_\xi\tilde{h}_\omega\frac{\partial\tilde{u}}{\partial\tilde{n}}\right) \qquad (3)$$

$$\frac{\tilde{u}}{\tilde{h}_\xi}\frac{\partial\tilde{w}}{\partial\tilde{\xi}} + \frac{\tilde{w}}{\tilde{h}_\omega}\frac{\partial\tilde{w}}{\partial\tilde{\omega}} + \tilde{v}\frac{\partial\tilde{w}}{\partial\tilde{n}} + \frac{\tilde{u}\tilde{w}}{\tilde{h}_\xi\tilde{h}_\omega}\frac{\partial\tilde{h}_\omega}{\partial\tilde{\xi}} - \frac{\tilde{u}^2}{\tilde{h}_\xi\tilde{h}_\omega}\frac{\partial\tilde{h}_\xi}{\partial\tilde{\omega}} + \frac{\tilde{w}\tilde{v}}{\tilde{h}_\omega}\frac{\partial\tilde{h}_\omega}{\partial\tilde{n}}$$

$$= -\frac{1}{\tilde{h}_\omega}\frac{\partial\tilde{p}}{\partial\tilde{\omega}} + \frac{Re^{-1}}{\tilde{h}_\xi\tilde{h}_\omega}\frac{\partial}{\partial\tilde{\xi}}\left(\frac{\tilde{h}_\omega}{\tilde{h}_\xi}\frac{\partial\tilde{w}}{\partial\tilde{\xi}}\right) + \frac{Re^{-1}}{\tilde{h}_\xi\tilde{h}_\omega}\frac{\partial}{\partial\tilde{\omega}}\left(\frac{\tilde{h}_\xi}{\tilde{h}_\omega}\frac{\partial\tilde{w}}{\partial\tilde{\omega}}\right)$$

$$+ \frac{Re^{-1}}{\tilde{h}_\xi\tilde{h}_\omega}\frac{\partial}{\partial\tilde{n}}\left(\tilde{h}_\xi\tilde{h}_\omega\frac{\partial\tilde{w}}{\partial\tilde{n}}\right) \qquad (4)$$

$$\frac{\tilde{u}}{\tilde{h}_\xi}\frac{\partial\tilde{v}}{\partial\tilde{\xi}} + \frac{\tilde{w}}{\tilde{h}_\omega}\frac{\partial\tilde{v}}{\partial\tilde{\omega}} + \tilde{v}\frac{\partial\tilde{v}}{\partial\tilde{n}} - \frac{\tilde{u}^2}{\tilde{h}_\xi}\frac{\partial\tilde{h}_\xi}{\partial\tilde{n}} - \frac{\tilde{w}^2}{\tilde{h}_\omega}\frac{\partial\tilde{h}_\omega}{\partial\tilde{n}} = -\frac{\partial\tilde{p}}{\partial\tilde{n}}$$

$$+ \frac{Re^{-1}}{\tilde{h}_\xi\tilde{h}_\omega}\frac{\partial}{\partial\tilde{\xi}}\left(\frac{\tilde{h}_\omega}{\tilde{h}_\xi}\frac{\partial\tilde{v}}{\partial\tilde{\xi}}\right) + \frac{Re^{-1}}{\tilde{h}_\xi\tilde{h}_\omega}\frac{\partial}{\partial\tilde{\omega}}\left(\frac{\tilde{h}_\xi}{\tilde{h}_\omega}\frac{\partial\tilde{v}}{\partial\tilde{\omega}}\right) + \frac{Re^{-1}}{\tilde{h}_\xi\tilde{h}_\omega}\frac{\partial}{\partial\tilde{n}}\left(\tilde{h}_\xi\tilde{h}_\omega\frac{\partial\tilde{v}}{\partial\tilde{n}}\right)$$

(5)

Energy

$$\frac{\tilde{u}}{\tilde{h}_\xi}\frac{\partial\tilde{T}}{\partial\tilde{\xi}} + \frac{\tilde{w}}{\tilde{h}_\omega}\frac{\partial\tilde{T}}{\partial\tilde{\omega}} + \tilde{v}\frac{\partial\tilde{T}}{\partial\tilde{n}} = \frac{Re^{-1}}{Pr\tilde{h}_\xi\tilde{h}_\omega}\left[\frac{\partial}{\partial\tilde{\xi}}\left(\frac{\tilde{h}_\omega}{\tilde{h}_\xi}\frac{\partial\tilde{T}}{\partial\tilde{\xi}}\right) + \frac{\partial}{\partial\tilde{\omega}}\left(\frac{\tilde{h}_\xi}{\tilde{h}_\omega}\frac{\partial\tilde{T}}{\partial\tilde{\omega}}\right)\right.$$

$$\left. + \frac{\partial}{\partial\tilde{n}}\left(\tilde{h}_\xi\tilde{h}_\omega\frac{\partial\tilde{T}}{\partial\tilde{n}}\right)\right] + \tilde{\Phi} \qquad (6)$$

where

$$\tilde{\Phi} = 2\left[\frac{1}{\tilde{h}_\xi}\frac{\partial\tilde{u}}{\partial\tilde{\xi}} + \frac{\tilde{w}}{\tilde{h}_\xi\tilde{h}_\omega}\frac{\partial\tilde{h}_\xi}{\partial\tilde{\omega}} + \frac{\tilde{v}}{\tilde{h}_\xi}\frac{\partial\tilde{h}_\xi}{\partial\tilde{n}}\right]^2$$

$$+ 2\left[\frac{1}{\tilde{h}_\omega}\frac{\partial\tilde{w}}{\partial\tilde{\omega}} + \frac{\tilde{v}}{\tilde{h}_\omega}\frac{\partial\tilde{h}_\omega}{\partial\tilde{n}} + \frac{\tilde{u}}{\tilde{h}_\xi\tilde{h}_\omega}\frac{\partial\tilde{h}_\omega}{\partial\tilde{\xi}}\right]^2$$

$$+ 2\left(\frac{\partial\tilde{v}}{\partial\tilde{n}}\right)^2 + \left[\frac{1}{\tilde{h}_\omega}\frac{\partial\tilde{v}}{\partial\tilde{\omega}} + \tilde{h}_\omega\frac{\partial}{\partial\tilde{n}}\left(\frac{\tilde{w}}{\tilde{h}_\omega}\right)\right]^2$$

$$+ \left[\tilde{h}_\xi\frac{\partial}{\partial\tilde{n}}\left(\frac{\tilde{u}}{\tilde{h}_\xi}\right) + \frac{1}{\tilde{h}_\xi}\frac{\partial\tilde{v}}{\partial\tilde{\xi}}\right]^2 + \left[\frac{\tilde{h}_\omega}{\tilde{h}_\xi}\frac{\partial}{\partial\tilde{\xi}}\left(\frac{\tilde{w}}{\tilde{h}_\omega}\right) + \frac{\tilde{h}_\xi}{\tilde{h}_\omega}\frac{\partial}{\partial\tilde{\omega}}\left(\frac{\tilde{u}}{\tilde{h}_\xi}\right)\right]^2$$

$$+ \lambda\left[\frac{1}{\tilde{h}_\xi}\frac{\partial\tilde{u}}{\partial\tilde{\xi}} + \frac{1}{\tilde{h}_\omega}\frac{\partial\tilde{w}}{\partial\tilde{\omega}} + \frac{\partial\tilde{v}}{\partial\tilde{n}} + \frac{\tilde{w}}{\tilde{h}_\xi\tilde{h}_\omega}\frac{\partial\tilde{h}_\xi}{\partial\tilde{\omega}} + \frac{\tilde{v}}{\tilde{h}_\xi}\frac{\partial\tilde{h}_\xi}{\partial\tilde{n}}\right.$$

$$\left. + \frac{\tilde{v}}{\tilde{h}_\omega}\frac{\partial\tilde{h}_\omega}{\partial\tilde{n}} + \frac{\tilde{u}}{\tilde{h}_\xi\tilde{h}_\omega}\frac{\partial\tilde{h}_\omega}{\partial\tilde{\xi}}\right]^2 \qquad (7)$$

In the above equations the following non-dimensionalization has been introduced:

$$\tilde{u} = \frac{u^*}{U_\infty^*},\ \tilde{w} = \frac{w^*}{U_\infty^*},\ \tilde{v} = \frac{v^*}{U_\infty^*},\ \tilde{\xi} = \frac{\xi^*}{L^*},\ \tilde{\omega} = \omega^*,\ \tilde{n} = \frac{n^*}{L^*},\ \tilde{p} = \frac{p^*}{\rho^* U_\infty^{*2}}$$

$$\tilde{h}_\xi = h_\xi^*,\ \tilde{h}_\omega = \frac{h_\omega^*}{L^*},\ \tilde{T} = \frac{T^* C}{U_\infty^{*2}} \qquad (8)$$

We now approach the above equations with the assumption that in a vanishingly small region near the surface, a region of order ε thick, all flow properties except the normal velocity component are of order one - v itself being of order ε. Thus, we introduce the following stretched coordinates:

$$\bar{\xi} = \tilde{\xi},\ \bar{\omega} = \tilde{\omega},\ \bar{n} = \tilde{n}/\varepsilon \tag{9}$$

where $\varepsilon = Re^{-1/2}$. According to our above described ordering scheme we then write

$$\begin{aligned} u(\bar{\xi},\bar{\omega},\bar{n};\varepsilon) &= \tilde{u}(\tilde{\xi},\tilde{\omega},\tilde{n};\varepsilon) \\ w(\bar{\xi},\bar{\omega},\bar{n};\varepsilon) &= \tilde{w}(\tilde{\xi},\tilde{\omega},\tilde{n};\varepsilon) \\ v(\bar{\xi},\bar{\omega},\bar{n};\varepsilon) &= \varepsilon^{-1}\tilde{v}(\tilde{\xi},\tilde{\omega},\tilde{n};\varepsilon) \\ p(\bar{\xi},\bar{\omega},\bar{n};\varepsilon) &= \tilde{p}(\tilde{\xi},\tilde{\omega},\tilde{n};\varepsilon) \end{aligned} \tag{10}$$

and note that $\bar{h}_\xi = \tilde{h}_\xi$ and $\bar{h}_\omega = \tilde{h}_\omega$.

Introduction of Eq. (9) and (10) into the governing equations and retention of all terms to order ε gives

$$\frac{\partial(\bar{h}_\xi u)}{\partial\bar{\xi}} + \frac{\partial(\bar{h}_\omega w)}{\partial\bar{\omega}} \quad \frac{\partial(\bar{h}_\xi \bar{h}_\omega v)}{\partial\bar{n}} = 0 \tag{11}$$

$$\frac{u}{\bar{h}_\xi}\frac{\partial u}{\partial\bar{\xi}} + \frac{w}{\bar{h}_\omega}\frac{\partial u}{\partial\bar{\omega}} + v\frac{\partial u}{\partial\bar{n}} - \frac{w^2}{\bar{h}_\xi\bar{h}_\omega}\frac{\partial\bar{h}_\omega}{\partial\bar{\xi}} + \frac{uw}{\bar{h}_\xi\bar{h}_\omega}\frac{\partial\bar{h}_\xi}{\partial\bar{\omega}} + \frac{uv}{\bar{h}_\xi}\frac{\partial\bar{h}_\xi}{\partial\bar{n}}$$

$$= -\frac{1}{\bar{h}_\xi}\frac{\partial p}{\partial\bar{\xi}} + \frac{1}{\bar{h}_\xi\bar{h}_\omega}\frac{\partial}{\partial\bar{n}}\left(\frac{\bar{h}_\xi\bar{h}_\omega}{\partial\bar{n}}\frac{\partial u}{\partial\bar{n}}\right) \tag{12}$$

$$\frac{u}{\bar{h}_\xi}\frac{\partial w}{\partial \bar{\xi}} + \frac{w}{\bar{h}_\omega}\frac{\partial w}{\partial \bar{\omega}} + v\frac{\partial w}{\partial \bar{n}} + \frac{uw}{\bar{h}_\xi \bar{h}_\omega}\frac{\partial \bar{h}_\omega}{\partial \bar{\xi}} - \frac{u^2}{\bar{h}_\xi \bar{h}_\omega}\frac{\partial \bar{h}_\xi}{\partial \bar{\omega}} + \frac{wv}{\bar{h}_\omega}\frac{\partial \bar{h}_\omega}{\partial \bar{n}}$$

$$= -\frac{1}{\bar{h}_\omega}\frac{\partial p}{\partial \bar{\omega}} + \frac{1}{\bar{h}_\xi \bar{h}_\omega}\frac{\partial}{\partial \bar{n}}\left(\frac{\bar{h}_\xi \bar{h}_\omega}{}\frac{\partial w}{\partial \bar{n}}\right) \qquad (13)$$

$$\frac{u^2}{\bar{h}_\xi}\frac{\partial \bar{h}_\xi}{\partial \bar{n}} + \frac{w^2}{\bar{h}_\omega}\frac{\partial \bar{h}_\omega}{\partial \bar{n}} = \frac{\partial p}{\partial \bar{n}} \qquad (14)$$

$$\frac{u}{\bar{h}_\xi}\frac{\partial T}{\partial \bar{\xi}} + \frac{w}{\bar{h}_\omega}\frac{\partial T}{\partial \bar{\omega}} + v\frac{\partial T}{\partial \bar{n}} = \frac{1}{\bar{h}_\xi \bar{h}_\omega \mathrm{Pr}}\frac{\partial}{\partial \bar{n}}\left(\bar{h}_\xi \bar{h}_\omega \frac{\partial T}{\partial \bar{n}}\right)$$

$$+ \bar{h}_\xi^2\left[\frac{\partial}{\partial \bar{n}}\left(\frac{u}{\bar{h}_\xi}\right)\right]^2 + \bar{h}_\omega^2\left[\frac{\partial}{\partial \bar{n}}\left(\frac{w}{\bar{h}_\omega}\right)\right]^2 \qquad (15)$$

Equations (11) through (15) represent the full second-order three-dimensional incompressible boundary-layer equations written in the surface-oriented curvilinear coordinate system described above.

2. Boundary and Matching Conditions

In order to complete the above described set of equations, the boundary conditions at the body surface and matching conditions at the boundary-layer edge must be established.

At the wall we apply the usual no slip condition and write

$$u(\bar{\xi},\bar{\omega},0) = w(\bar{\xi},\bar{\omega},0) = 0 \tag{16}$$

To allow for mass injection at the surface we write

$$v(\bar{\xi},\bar{\omega},0) = v_0(\bar{\xi},\bar{\omega}) \tag{17}$$

Using the subscript m to denote matching values, we write for large n,

$$\left.\begin{aligned} u &\longrightarrow u_m(\bar{\xi},\bar{\omega},\bar{n}) \\ w &\longrightarrow w_m(\bar{\xi},\bar{\omega},\bar{n}) \\ p &\longrightarrow p_m(\bar{\xi},\bar{\omega},\bar{n}) \end{aligned}\right\} \quad \text{as } n \longrightarrow \infty \tag{18}$$

In order to find values for u_m and w_m we turn to the requirement of vanishing vorticity for large n. First we note that

$$\underline{\Omega} = \underline{\nabla} \times \underline{V} = \frac{1}{\tilde{h}_\xi \tilde{h}_\omega} \left\{ \tilde{h}_\xi \tilde{h}_\omega \tilde{i}_\xi \left[\frac{\partial \tilde{V}}{\partial \tilde{\omega}} - \frac{\partial (\tilde{h}_\omega \tilde{w})}{\partial \tilde{n}} \right] \right.$$

$$\left. - \tilde{h}_\omega \tilde{i}_\omega \left[\frac{\partial \tilde{V}}{\partial \tilde{\xi}} - \frac{\partial (\tilde{h}_\xi \tilde{u})}{\partial \tilde{n}} \right] + \tilde{i}_n \left[\frac{\partial (\tilde{h}_\omega \tilde{w})}{\partial \tilde{\xi}} - \frac{\partial (\tilde{h}_\xi \tilde{u})}{\partial \tilde{\omega}} \right] \right\}$$

Substituting Eqs. (9) and (10), the boundary-layer scaling laws gives

$$\underline{\Omega} = \frac{1}{\bar{h}_\xi \bar{h}_\omega} \left\{ \bar{h}_\xi \bar{i}_\xi \left[\varepsilon \frac{\partial V}{\partial \bar{w}} - \frac{1}{\varepsilon} \frac{\partial (\bar{h}_\omega w)}{\partial \bar{n}} \right] - \bar{h}_\omega \bar{i}_\omega \left[\varepsilon \frac{\partial V}{\partial \bar{\xi}} - \frac{1}{\varepsilon} \frac{\partial (\bar{h}_\xi u)}{\partial \bar{n}} \right] \right.$$

$$+ \varepsilon \bar{i}_n \left[\frac{\partial(\bar{h}_\omega w)}{\partial \bar{\xi}} - \frac{\partial(\bar{h}_\xi u)}{\partial \bar{\omega}} \right] \Bigg\}$$

Multiplying by ε and retaining terms to $O(\varepsilon)$ gives

$$\varepsilon \underline{\Omega} = - \frac{\bar{i}_\xi}{\bar{h}_\omega} \frac{\partial(\bar{h}_\omega w)}{\partial \bar{n}} + \frac{\bar{i}_\omega}{\bar{h}_\xi} \frac{\partial(\bar{h}_\xi u)}{\partial \bar{n}}$$

Requiring $\underline{\Omega}$ to vanish at large $\bar{n}$ then gives

$$\left.\begin{aligned} \frac{\partial(\bar{h}_\omega w)}{\partial \bar{n}} &= 0 \\ \frac{\partial(\bar{h}_\xi u)}{\partial \bar{n}} &= 0 \end{aligned}\right\} \quad \text{as } \bar{n} \longrightarrow \infty \qquad (19)$$

Equations (19) can be integrated to give

$$\left.\begin{aligned} u_m &= \frac{F_1(\bar{\xi}, \bar{\omega})}{\bar{h}_\xi} \\ w_m &= \frac{F_2(\bar{\xi}, \bar{\omega})}{\bar{h}_\omega} \end{aligned}\right\} \quad \text{as } \bar{n} \longrightarrow \infty \qquad (20)$$

In order to establish F_1 and F_2 the matching condition that the viscous velocity profile as $\bar{n} \longrightarrow \infty$ match the inviscid velocity profile as $\tilde{n} \longrightarrow 0$ will be used. Thus

$$\left.\begin{aligned} u_m &= \frac{F_1(\bar{\xi}, \bar{\omega})}{\bar{h}_\xi} \sim U(\tilde{\xi}, \tilde{\omega}, \tilde{n}) \\ w_m &= \frac{F_2(\bar{\xi}, \bar{\omega})}{\bar{h}_\omega} \sim W(\tilde{\xi}, \tilde{\omega}, \tilde{n}) \end{aligned}\right\} \quad \text{as } \tilde{n} \longrightarrow 0 \qquad (21)$$

where the capitol letters denote inviscid quantities. Expanding the first of Eqs. (21) in a MacLaurin series gives

$$\frac{F_1(\bar{\xi},\bar{\omega})}{\bar{h}_\xi} = U(\bar{\xi},\bar{\omega},0) + \left(\frac{\partial U}{\partial \tilde{n}}\right)_{\bar{\xi},\bar{\omega},0} \tilde{n} + \ldots$$

The outer flow must be irrotational, however, so that from the definition of vorticity

$$\frac{\partial(\tilde{h}_\xi U)}{\partial \tilde{n}} = \frac{\partial V}{\partial \tilde{\xi}}$$

or,

$$\frac{\partial U}{\partial \tilde{n}} = \frac{1}{\tilde{h}_\xi}\frac{\partial V}{\partial \tilde{\xi}} - \frac{U}{\tilde{h}_\xi}\frac{\partial \tilde{h}_\xi}{\partial \tilde{n}} = \frac{1}{\tilde{h}_\xi}\left[\frac{\partial V}{\partial \tilde{\xi}} - U\frac{\partial \tilde{h}_\xi}{\partial \tilde{n}}\right]$$

We now note that, by a MacLaurin series,

$$(\tilde{h}_\xi)_{\tilde{\xi},\tilde{\omega},\tilde{n}} = (\tilde{h}_\xi)_{\tilde{\xi},\tilde{\omega},0} + \left(\frac{\partial \tilde{h}_\xi}{\partial \tilde{n}}\right)_{\tilde{\xi},\tilde{\omega},0} \tilde{n} + \ldots$$

$$= \tilde{h}_{\xi,0} + \left(\frac{\partial \tilde{h}_\xi}{\partial \tilde{n}}\right)_0 \tilde{n} + \ldots$$

$$= \tilde{h}_{\xi,0}\,(1 + \tilde{k}_\xi\,\tilde{n} + \ldots)$$

Thus, using the binomial series

$$\frac{F_1(\bar{\xi},\bar{\omega})}{\tilde{h}_{\xi,0}}(1 - \tilde{k}_\xi\tilde{n} + \tilde{k}_\xi^2\tilde{n}^2) = U(\tilde{\xi},\tilde{\omega},0)(1 - \tilde{k}_\xi\tilde{n} + \tilde{k}_\xi^2\,\tilde{n}^2) + \ldots$$

where the boundary condition $V(\tilde{\xi},\tilde{\omega},0) = 0$ has been used. Finally

$$F_1(\bar{\xi},\bar{\omega}) = \tilde{h}_{\xi,0}\,U(\tilde{\xi},\tilde{\omega},0). \tag{22}$$

In a similar manner

$$F_2(\bar{\xi},\bar{\omega}) = \tilde{h}_{\omega,0}\,W(\tilde{\xi},\tilde{\omega},0) \tag{23}$$

Equations (20) then become

$$\left.\begin{aligned} u_m &= \frac{\bar{h}_{\xi,0}\,U(\tilde{\xi},\tilde{\omega},0)}{\bar{h}_\xi} \\ w_m &= \frac{\bar{h}_{\omega,0}\,W(\tilde{\xi},\tilde{\omega},0)}{\bar{h}_\omega} \end{aligned}\right\} \text{ as } \bar{n}\longrightarrow\infty \tag{24}$$

since $\bar{h}_\xi = \tilde{h}_\xi$ and $\bar{h}_\omega = \tilde{h}_\omega$.

3. Elimination of Pressure from the Boundary-Layer Equations

Examination of Eqs. (11) through (15) reveals that the principle difference between these equations and the usual first-order boundary-layer equations is the fact that the pressure is not constant across the layer. As pointed out in Ref. 6 for the two-dimensional case, these equations can be made similar to the first-order boundary-layer equations by eliminating the pressure as a variable, hence eliminating the need for direct solution of the normal momentum equation. Once this is

accomplished, solution procedures similar to those for the first-order equations (see Refs. 2 and 6) may be applied to the system.

In order to eliminate the pressure the normal momentum equation, Eq. (14) is first integrated to give

$$p(\bar{\xi},\bar{\omega},\bar{n}) = -\int_0^{\bar{n}} \frac{\bar{h}_{\xi,n}}{\bar{h}_\xi^3}\left(\bar{h}_{\xi,0}^2\, U_e^2 - \bar{h}_\xi^2 u^2\right) d\bar{n}'$$

$$-\int_0^{\bar{n}} \frac{\bar{h}_{\omega,n}}{\bar{h}_\omega^3}\left(\bar{h}_{\omega,0}^2\, W_e^2 - \bar{h}_\omega^2\, w^2\right) d\bar{n}'$$

$$-\frac{\bar{h}_{\xi,0}^2 U_e^2}{2\bar{h}_\xi^2} - \frac{\bar{h}_{\omega,0}^2 W_e^2}{2\bar{h}_\omega^2} + \bar{F}(\bar{\xi},\bar{\omega}) \qquad (25)$$

where use has been made of the matching conditions. Now note that

$$I_{\bar{\xi}}(\bar{n}_1,\bar{n}_2) = -\int_{\bar{n}_1}^{\bar{n}_2} \frac{\bar{h}_{\xi,n}}{\bar{h}_\xi^3}\left(\bar{h}_{\xi,0}^2\, U_e^2 - \bar{h}_\xi^2\, u^2\right) d\bar{n}' \qquad (26)$$

$$I_{\bar{\omega}}(\bar{n}_1,\bar{n}_2) = -\int_{\bar{n}_1}^{\bar{n}_2} \frac{\bar{h}_{\omega,n}}{\bar{h}_\omega^3}\left(\bar{h}_{\omega,0}^2\, W_e^2 - \bar{h}_\omega^2\, w^2\right) d\bar{n}' \qquad (27)$$

Eq. (25) is differentiated with respect to $\bar{\omega}$ and evaluated at $\bar{n}\to\infty$ to give

$$\frac{\partial \bar{F}}{\partial \bar{\omega}} = \frac{\partial\left[I_{\bar{\xi}}^{-}(0,\bar{n}) + I_{\bar{\omega}}^{-}(0,\bar{n})\right]}{\partial \bar{\omega}} + \frac{\partial}{\partial \bar{\omega}}\left(\frac{\bar{h}_{\xi,0}^{2} U_e^2}{2\bar{h}_{\xi}^{2}}\right) + \frac{\partial}{\partial \bar{\omega}}\left(\frac{\bar{h}_{\omega,0}^{2} W_e^2}{2\bar{h}_{\omega}^{2}}\right) + \frac{\partial P}{\partial \omega} \tag{28}$$

In order to evaluate $\partial p/\partial\bar{\omega}$ as $\bar{n}\to\infty$ the $\bar{n}\to\infty$ limit of Eq. (13) is taken, which gives, after use of the matching and inviscid irrotationality condition

$$-\frac{\partial p}{\partial \bar{\omega}} = \frac{1}{2}\frac{\partial}{\partial \bar{\omega}}\left[\left(\frac{\bar{h}_{\xi,0} U_e}{\bar{h}_{\xi}}\right)^2 + \left(\frac{\bar{h}_{\omega,0} W_e}{\bar{h}_{\omega}}\right)^2\right]$$

Use of this result in Eq. (28) then gives

$$\frac{\partial \bar{F}}{\partial \bar{\omega}} = \frac{\partial (I_{\bar{\xi}}^{-} + I_{\bar{\omega}}^{-})}{\partial \bar{\omega}}$$

or, upon integration

$$\bar{F} = I_{\bar{\xi}}^{-} + I_{\bar{\omega}}^{-} + \tilde{F}(\bar{\xi})$$

Thus, Eq. (25) becomes

$$p(\bar{\xi},\bar{\omega},\bar{n}) = \int_{\bar{n}}^{\infty} \frac{\bar{h}_{\xi,n}}{\bar{h}_{\xi}^{3}}\left(\bar{h}_{\xi,0}^{2} U_e^2 - \bar{h}_{\xi}^{2} u^2\right) d\bar{n}' + \int_{\bar{n}}^{\infty} \frac{\bar{h}_{\omega,n}}{\bar{h}_{\omega}^{3}}\left(\bar{h}_{\omega,0}^{2} W_e^2 - \bar{h}_{\omega}^{2} w^2\right) d\bar{n}' + \tilde{F}(\bar{\xi}) \tag{29}$$

In a similar manner, this equation is differentiated with respect to $\bar{\xi}$ and evaluated as $\bar{n} \longrightarrow \infty$ yielding

$$\frac{\partial \tilde{F}}{\partial \bar{\xi}} = \frac{\partial p}{\partial \bar{\xi}} \tag{30}$$

Evaluating Eq. (12) as $\bar{n} \longrightarrow \infty$ and using the matching and irrotationality conditions gives

$$\frac{\partial p}{\partial \bar{\xi}} = -\frac{1}{2}\frac{\partial}{\partial \bar{\xi}}\left[\left(\frac{\bar{h}_{\xi,0}U_e}{\bar{h}_\xi}\right)^2 + \left(\frac{\bar{h}_{\omega,0}W_e}{\bar{h}_\omega}\right)^2\right]$$

so that

$$\frac{\partial \tilde{F}}{\partial \bar{\xi}} = -\frac{1}{2}\frac{\partial}{\partial \bar{\xi}}\left[\left(\frac{\bar{h}_{\xi,0}U_e}{\bar{h}_\xi}\right)^2 + \left(\frac{\bar{h}_{\omega,0}W_e}{\bar{h}_\omega}\right)^2\right]$$

Integration of this result with respect to $\bar{\xi}$ and substitution into Eq. (29) gives

$$p(\bar{\xi},\bar{\omega},\bar{n}) = \int_{\bar{n}}^{\infty} \frac{\bar{h}_{\xi,n}}{\bar{h}_\xi^3}\left(\bar{h}_{\xi,0}^2 U_e^2 - \bar{h}_\xi^2 u^2\right) d\bar{n}' + \int_{\bar{n}}^{\infty} \frac{\bar{h}_{\omega,n}}{\bar{h}_\omega^3}\left(\bar{h}_{\omega,0}^2 W_e^2 - \bar{h}_\omega^2 w^2\right) d\bar{n}' - \frac{\bar{h}_{\xi,0}^2 U_e^2}{2\bar{h}_\xi^2} - \frac{\bar{h}_{\omega,0}^2 W_e^2}{2\bar{h}_\omega^2} + C \tag{31}$$

where C is a constant of integration. In order to evaluate C Eq. (31) is examined as $\bar{n}\to\infty$,

$$p_m(\bar{\xi},\bar{\omega}) = -\frac{\bar{h}_{\xi,0}^2 U_e^2}{2\bar{h}_\xi^2} - \frac{\bar{h}_{\omega,0} W_e^2}{2\bar{h}_\omega^2} + C \tag{32}$$

From inviscid conditions near the body,

$$P_e = -\frac{W_e^2}{2} - \frac{U_e^2}{2} + C$$

which is recognized as Bernoulli's equation and hence C is identified as the stagnation pressure. Solving Eq. (32) for C and substituting into Eq. (31) yields

$$p(\bar{\xi},\bar{\omega},\bar{n}) = P_e(\bar{\xi},\bar{\omega}) + \frac{U_e^2}{2}\left(1 - \frac{\bar{h}_{\xi,0}^2}{\bar{h}_\xi^2}\right)$$

$$+ \frac{W_e^2}{2}\left(1 - \frac{\bar{h}_{\omega,0}^2}{\bar{h}_\omega^2}\right) + I_{\bar{\xi}}(\bar{n},\infty) + I_{\bar{\omega}}(\bar{n},\infty) \tag{33}$$

The pressure is finally eliminated from Eqs. (12) and (13) by substitution of Eq. (33) which gives

$$\frac{u}{\bar{h}_\xi}\frac{\partial u}{\partial\bar{\xi}} + \frac{w}{\bar{h}_\omega}\frac{\partial u}{\partial\bar{\omega}} + v\frac{\partial u}{\partial\bar{n}} - \frac{w^2}{\bar{h}_\xi\bar{h}_\omega}\frac{\partial\bar{h}_\omega}{\partial\bar{\xi}} + \frac{uw}{\bar{h}_\xi\bar{h}_\omega}\frac{\partial\bar{h}_\xi}{\partial\bar{\omega}}$$

$$+ \frac{uv}{\bar{h}_\xi}\frac{\partial\bar{h}_\xi}{\partial\bar{n}} + \frac{1}{\bar{h}_\xi}\frac{\partial}{\partial\bar{\xi}}(I_{\bar{\xi}} + I_{\bar{\omega}})$$

$$= -\frac{1}{\bar{h}_\xi}\frac{\partial Q}{\partial\bar{\xi}} + \frac{1}{\bar{h}_\xi\bar{h}_\omega}\frac{\partial}{\partial\bar{n}}\left(\bar{h}_\xi\bar{h}_\omega\frac{\partial u}{\partial\bar{n}}\right) \tag{34}$$

$$\frac{u}{\bar{h}_\xi}\frac{\partial w}{\partial \bar{\xi}} + \frac{w}{\bar{h}_\omega}\frac{\partial w}{\partial \bar{\omega}} + v\frac{\partial w}{\partial \bar{n}} + \frac{uw}{\bar{h}_\xi \bar{h}_\xi}\frac{\partial \bar{h}_\omega}{\partial \bar{\xi}} - \frac{u^2}{\bar{h}_\xi \bar{h}_\omega}\frac{\partial \bar{h}_\xi}{\partial \bar{\omega}}$$

$$+ \frac{wv}{\bar{h}_\omega}\frac{\partial \bar{h}_\omega}{\partial \bar{n}} + \frac{1}{\bar{h}_\omega}\frac{\partial}{\partial \bar{\omega}}(I_{\bar{\xi}} + I_{\bar{\omega}}) = -\frac{1}{\bar{h}_\omega}\frac{\partial Q}{\partial \bar{\omega}}$$

$$+ \frac{1}{\bar{h}_\xi \bar{h}_\omega}\frac{\partial}{\partial \bar{n}}\left(\bar{h}_\xi \bar{h}_\omega \frac{\partial w}{\partial \bar{n}}\right) \tag{35}$$

where

$$Q = -\frac{\bar{h}^2_{\xi,0}U_e^2}{2\bar{h}^2_\xi} - \frac{\bar{h}^2_{\omega,0}W_e^2}{2\bar{h}^2_\omega} \tag{36}$$

4. Transformation of the Boundary-Layer Equations

We now define the following new independent variables

$$\left.\begin{aligned} \xi &= \bar{\xi} \\ \omega &= \bar{\omega} \\ \eta(\bar{\xi},\bar{\omega},\bar{n}) &= \sqrt{\frac{2U_e}{\xi}}\ \bar{n} \end{aligned}\right\} \tag{37}$$

and new dependent variables

$$\left.\begin{aligned} F &= \frac{h_\xi u}{\bar{h}_{\xi,0}U_e} \\ G &= \frac{h_\omega w}{\bar{h}_{\omega,0}W} \\ \Theta &= T/T_e \end{aligned}\right\} \tag{38}$$

where W can be either W_e or U_e. From the chain rule

$$\left.\begin{aligned} \frac{\partial}{\partial \bar{\xi}} &= \frac{\partial}{\partial \xi} + \eta_{\bar{\xi}}\frac{\partial}{\partial \eta} \\ \frac{\partial}{\partial \bar{\omega}} &= \frac{\partial}{\partial \omega} + \eta_{\bar{\omega}}\frac{\partial}{\partial \eta} \\ \frac{\partial}{\partial \bar{n}} &= \sqrt{\frac{2U_e}{\xi}}\ \frac{\partial}{\partial \eta} \end{aligned}\right\} \tag{39}$$

The time averaged continuity equation, Eq. (11), is now integrated to give

$$v = -\frac{1}{\bar{h}_\xi \bar{h}_\omega}\frac{\partial}{\partial \bar{\xi}}\int_0^{\bar{n}} \bar{h}_\omega u d\bar{n}' - \frac{1}{\bar{h}_\xi \bar{h}_\omega}\frac{\partial}{\partial \bar{\omega}}\int_0^{\bar{n}} \bar{h}_\xi w d\bar{n}'$$

or, after using Eqs. (37) through (39)

$$\sqrt{\frac{2}{U_e \xi}}\, v = \frac{2}{\xi} V - \frac{h_{\xi,0} F}{h_\xi^2}\eta_{\bar{\xi}} - \frac{h_{\omega,0} GW}{h_\omega^2 U_e}\eta_{\bar{\omega}} \tag{40}$$

where

$$V = \frac{\xi}{2}\left[\sqrt{\frac{2}{U_e \xi}}\, v - \frac{h_{\xi,0} F}{h_\xi^2}\eta_{\bar{\xi}} - \frac{h_{\omega,0} GW}{h_\omega^2 U_e}\eta_{\bar{\omega}}\right] \tag{41}$$

This equation is now differentiated with respect to η to give

$$V_\eta = -\frac{1}{h_\xi h_\omega}\sqrt{\frac{\xi}{2U_e}}\left[\frac{\partial}{\partial \xi}\left(\frac{h_\omega h_{\xi,0}}{h_\xi}\sqrt{\frac{\xi}{2U_e}}\, U_e F\right)\right.$$

$$\left. + \frac{\partial}{\partial \omega}\left(\frac{h_\xi h_{\omega,0}}{h_\omega}\sqrt{\frac{\xi}{2U_e}}\, WG\right) - V\frac{\partial (h_\xi^{-1} h_\omega^{-1})}{\partial \eta}\right] \tag{42}$$

which is the transformed continuity equation.

The convective operator is now transformed,

$$\frac{u}{\bar{h}_\xi}\frac{\partial}{\partial \bar{\xi}} + \frac{w}{\bar{h}_\omega}\frac{\partial}{\partial \bar{\omega}} + v\frac{\partial}{\partial \bar{n}} = \frac{h_{\xi,0} U_e F}{h_\xi^2}\frac{\partial}{\partial \xi} + \frac{h_{\xi,0} U_e F}{h_\xi^2}\eta_{\bar{\xi}}\frac{\partial}{\partial \eta}$$

$$+ \frac{h_{\omega,0} WG}{h_\omega^2}\frac{\partial}{\partial \omega} + \frac{h_{\omega,0} WG}{h_\omega^2}\eta_{\bar{\omega}}\frac{\partial}{\partial \eta} + v\sqrt{\frac{2U_e}{\xi}}\frac{\partial}{\partial \eta}$$

Using Eq. (40) this result becomes

$$\frac{u}{\bar{h}_\xi}\frac{\partial}{\partial\bar{\xi}} + \frac{w}{\bar{h}_\omega}\frac{\partial}{\partial\bar{\omega}} + v\frac{\partial}{\partial\bar{n}} = \frac{h_{\xi,0}U_e F}{h_\xi^2}\frac{\partial}{\partial\xi} + \frac{h_{\omega,0}WG}{h_\omega^2}\frac{\partial}{\partial\omega} + \frac{2U_e}{\xi}V\frac{\partial}{\partial\eta} \qquad (43)$$

The transformation relations, Eqs. (37), (38), (39) and (43) are now applied to the time averaged $\bar{\xi}$ momentum equation, Eq. (34) yielding

$$h_{\xi,0}\frac{\xi F}{2h_\xi^2}F_\xi + \frac{\xi\bar{\alpha}_2 G}{2h_\omega}\left(\frac{h_{\omega,0}}{h_\omega}\right)F_\omega + (V + \sigma H_m + \sigma_\eta)F_\eta = \sigma F_{\eta\eta}$$

$$+ \frac{1}{2}\left(\frac{h_{\xi,0}}{h_\xi}\right)^2\beta_1(1-F^2) + \frac{1}{2}\left(\frac{h_{\omega,0}}{h_\omega}\right)^2(\beta_2 + \xi K_{\xi,0})$$

$$(\bar{\alpha}_1 - \bar{\alpha}_2 FG) - \frac{\xi}{2}(1-F^2)(L_\xi - L_{\xi,0}) - \frac{\xi\bar{\alpha}_2^2}{2}$$

$$\left(\frac{h_\xi}{h_{\xi,0}}\right)\left(\frac{h_{\omega,0}}{h_\omega}\right)^2(\bar{\alpha}_3^2 - G^2)K_\omega - \frac{\sigma F}{h_\xi h_\omega}\frac{\partial h_\omega}{\partial\eta}\frac{\partial h_\xi}{\partial\eta}$$

$$+ \frac{\sigma F}{h_\xi^2}\left(\frac{\partial h_\xi}{\partial\eta}\right)^2 - \frac{\sigma F}{h_\xi}\frac{\partial^2 h_\xi}{\partial\eta^2} + F\sigma_\eta\frac{h_{\xi,\eta}}{h_\xi} + \frac{\xi A}{2h_{\xi,0}U_e^2}\eta_{\bar{\xi}}$$

$$- \frac{\xi}{\partial h_{\xi,0}U_e^2}\frac{\partial}{\partial\xi}(I_\xi + I_\omega) \qquad (44)$$

where

$$I_\xi = \int_{\bar{n}}^{\infty}\frac{\bar{h}_{\xi,0}}{\bar{h}_\xi}(\bar{h}_{\xi,0}U_e^2 - \bar{h}_\xi u^2)d\bar{n}'$$

$$= \int_\eta^\infty \frac{h_{\xi,0}}{h_\xi^3}h_{\xi,0}^2U_e^2(1-F^2)\sqrt{\frac{\xi}{2U_e}}\,d\eta'$$

$$= \sqrt{\frac{U_e^3\xi}{2}}\int_\eta^\infty\left(\frac{h_{\xi,0}}{h_\xi}\right)^3(1-F^2)d\eta' \qquad (45)$$

and

$$I_\omega = \int_{\bar{\eta}}^{\infty} \frac{\bar{h}_{\omega,0}}{\bar{h}_\omega^3} \left(\bar{h}_{\omega,0}^2 W_e^2 - \bar{h}_\omega^2 w^2\right) d\bar{\eta}'$$

$$= \int_{\eta}^{\infty} \frac{h_{\omega,0}}{h_\omega^3} h_{\omega,0}^2 W^2 \left(\frac{W_e^2}{W^2} - G^2\right) \sqrt{\frac{\xi}{2U_e}}\, d\eta' \qquad (46)$$

$$= W^2 \sqrt{\frac{\xi}{2U_e}} \int_{\eta}^{\infty} \left(\frac{h_{\omega,0}}{h_\omega}\right)^3 \left(\frac{W_e^2}{W^2} - G^2\right) d\eta'$$

Also,

$$A = \left[- \frac{h_{\omega,0}^2 W_e^2 \left(\frac{W_e^2}{W^2} - G^2\right)}{h_\omega^3} \frac{\partial h_\omega}{\partial \eta} - \frac{h_{\xi,0}^2 U_e^2 (1-F^2)}{h_\xi^3} \frac{\partial h_\xi}{\partial \eta} \right.$$

$$\left. - \left(\frac{h_{\xi,0}}{h_\xi}\right)^3 \sqrt{\frac{U_e^3 \xi}{2}} (1-F^2) - \left(\frac{h_{\omega,0}}{h_\omega}\right)^3 W^2 \sqrt{\frac{\xi}{2U_e}} \left(\frac{W_e^2}{W^2} - G^2\right) \right] \qquad (47)$$

In the following definitions, note that $W = U_e$ for general points and $W = W_e$ for the stagnation point and points on the symmetry planes.

$$\bar{\alpha}_1 = \frac{W_e}{U_e}\,, \quad \bar{\alpha}_2 = \frac{W}{U_e}\,, \quad \bar{\alpha}_3 = \frac{W_e}{W} \qquad (48)$$

$$\beta_1 = \frac{\xi}{h_{\xi,0} U_e} \frac{\partial U_e}{\partial \xi}, \quad \beta_2 = \frac{\xi}{h_{\omega,0} U_e} \frac{\partial U_e}{\partial \omega}\,, \quad \beta_3 = \frac{\xi}{h_{\xi,0} W_e} \frac{\partial W_e}{\partial \xi} \qquad (49)$$

$$K_\xi = \frac{1}{h_\xi h_\omega} \frac{\partial h_\xi}{\partial \omega}, \quad K_\omega = \frac{1}{h_\xi h_\omega} \frac{\partial h_\omega}{\partial \xi}, \quad L_\xi = \frac{h_{\xi,0}}{h_\xi^3} \frac{\partial h_\xi}{\partial \xi} \tag{50}$$

$$H_m = \left(\frac{1}{h_\xi} \frac{\partial h_\xi}{\partial \eta} - \frac{1}{h_\omega} \frac{\partial h_\omega}{\partial \eta} \right) \tag{51}$$

The transformation relations, Eqs. (37), (38), (39) and (42) when applied to the time averaged ω-momentum equation, Eq. (35), give

$$\frac{h_{\xi,0} F}{2h_\xi^2} G_\xi + \frac{h_{\omega,0} \bar{\alpha}_2 G}{2h_\omega^2} G_\omega + (V - \sigma H_m + \sigma_\eta) G_\eta - \left[\frac{\sigma}{h_\omega} \right.$$

$$\left. + \left(\frac{h_{\xi,\eta} h_{\omega,\eta}}{h_\xi} - \frac{h_{\omega,\eta}^2}{h_\omega} + h_{\omega,\eta\eta} \right) - \sigma_\eta \frac{h_{\omega,\xi}}{h_\omega} \right] G$$

$$= \sigma G_{\eta\eta} + \frac{1}{2} \left(\frac{h_{\xi,0}}{h_\xi} \right)^2 (\bar{\alpha}_3 - FG) \beta_5$$

$$+ \frac{1}{2} \left(\frac{h_{\omega,0}}{h_\omega} \right)^2 (\bar{\alpha}_1 \bar{\alpha}_3 - \bar{\alpha}_2 G^2) \beta_6$$

$$- \frac{\xi}{2\bar{\alpha}_2} \left(\frac{h_{\omega,0}}{h_\omega} \right)^{-1} \left(\frac{h_{\xi,0}}{h_\xi} \right)^2 (1-F^2) K_\xi$$

$$+ \frac{\xi}{2} \left(\frac{h_{\xi,0}}{h_\xi} \right)^2 (\bar{\alpha}_3 - FG) K_{\omega,0}$$

$$- \frac{\xi\bar{\alpha}_2}{2}(\bar{\alpha}_3^2 - G^2)(L_\omega - L_{\omega,0}) + \frac{\xi}{2h_{\xi,0}}\left(\frac{h_{\xi,0}}{h_\xi}\right)^2 \bar{\alpha}_{3,\xi}$$

$$+ \frac{\xi\bar{\alpha}_1}{2h_{\omega,0}}\left(\frac{h_{\omega,0}}{h_\omega}\right)^2 \bar{\alpha}_{3,\omega} + \frac{A\xi\eta_{\bar{\omega}}}{2h_{\omega,0}U_e W}$$

$$- \frac{\xi}{2h_{\omega,0}U_e W}\frac{\partial}{\partial\omega}(I_\xi + I_\omega) \tag{52}$$

where

$$\beta_4 = \frac{\xi}{h_{\omega,0}W_e}\frac{\partial W_e}{\partial\omega},\quad \beta_5 = \frac{\xi}{h_{\xi,0}W}\frac{\partial W}{\partial\xi},\quad \beta_6 = \frac{\xi}{h_{\omega,0}W}\frac{\partial W}{\partial\omega} \tag{53}$$

$$L_\omega = \frac{h_{\omega,0}}{h_\omega^3}\frac{\partial h_\omega}{\partial\omega} \tag{54}$$

Finally, the transformed time averaged energy equation is

$$\frac{h_{\xi,0}\xi F}{h_\xi^2}\theta_\xi + \frac{h_{\omega,0}\xi\bar{\alpha}_2 G}{h_\omega^2}\theta_\omega + (V+H_\theta)\theta_\eta = Pr^{-1}\theta_{\eta\eta} + h_{\xi,0}^2\lambda F_\eta^2 + h_{\omega,0}^2\lambda G_\eta^2\bar{\alpha}_2^2$$

$$- \frac{4h_{\xi,0}^2\lambda}{h_\xi^4}h_{\xi,\eta}^2 - \frac{4h_{\omega,0}^2\lambda\bar{\alpha}_2^2}{h_\omega^4}h_{\omega,\eta}^2 \tag{55}$$

where

$$H_\theta = \frac{1}{h_\omega}\frac{\partial h_\xi}{\partial\eta} + \frac{1}{h_\xi}\frac{\partial h_\xi}{\partial\eta},\quad \lambda = \frac{U_e^2}{T_e} \tag{56}$$

5. Transformed Governing Equations in the Plane of Symmetry

The governing equations at the windward symmetry plane are found by examining Eqs. (37) - (56) in the limit as $\omega \longrightarrow 0$. In the plane of symmetry we take $W = W_e$ and note that

$$G = \lim_{\omega \longrightarrow 0} \frac{w}{W_e} = \lim_{\omega \longrightarrow 0} \left[\frac{\left(\frac{\partial w}{\partial \omega}\right)}{\left(\frac{\partial W_e}{\partial \omega}\right)} \right] \tag{57}$$

with the last limit being bounded. In the plane of symmetry we note the following,

$$\bar{\alpha}_1 = \bar{\alpha}_2 = \frac{W_e}{U_e} = 0 \tag{58}$$

$$U_e = U_{e_1} + U_{e_2}\omega^2 + \ldots \tag{59}$$

$$W_e = W_{e_1}\,\omega + \ldots \tag{60}$$

$$h_\xi = H_1 + H_2\omega^2 + \ldots \tag{61}$$

$$h_\omega = H_\omega + \ldots \tag{62}$$

Substitution of Eqs. (58) to (62) into Eq. (42) gives

$$V_\eta = -\frac{1}{h_\xi h_\omega}\sqrt{\frac{\xi}{2U_e}}\left[\frac{\partial}{\partial \xi}\left(\frac{h_\omega h_{\xi,0}}{h_\xi}\sqrt{\frac{\xi}{2U_e}}\,U_e F\right)\right.$$

$$\left. + \frac{h_\xi h_{\omega,0} G}{h_\omega}\sqrt{\frac{\xi}{2U_e}}\,\frac{\partial W_e}{\partial \omega} - V\,\frac{\partial (h_\xi^{-1}\, h_\eta^{-1})}{\partial \eta}\right] \tag{63}$$

which is the windward streamline form of the continuity equation. We further note that at the symmetry plane $K_\xi = 0$, so that the ξ-momentum equation, Eq. (44), becomes

$$\sigma F_{\eta\eta} - (V + \sigma H_m + \sigma_\eta) F_\eta - \left[(1-V) \frac{h_{\xi,\eta}}{h_\xi} + \sigma M_\xi \right.$$

$$\left. - \sigma_\eta \frac{h_{\xi,\eta}}{h_\xi} \right] F - \frac{\xi F}{2h_\xi^2} F_\xi$$

$$= - \frac{1}{2} \left(\frac{h_{\xi,0}}{h_\xi} \right)^2 (1-F^2) \beta_1 + \frac{\xi}{2} (1-F^2)(L_\xi - L_{\xi,0})$$

$$- \frac{\xi A}{2h_{\xi,0} U_e^2} \eta_{\bar{\xi}} + \frac{\xi}{2h_{\xi,0} U_e^2} \frac{\partial (I_\xi + I_\omega)}{\partial \xi} \qquad (64)$$

Before examining the ω-momentum equation we must first look at some limits at the windward streamline,

$$\bar{\alpha}_1 \beta_6 = \bar{\alpha}_2 \beta_6 = \frac{\xi W_{e_1}}{h_{\omega,0} U_e} \qquad (65)$$

$$\frac{K_\xi}{\bar{\alpha}_2} = \frac{H_2 U_e}{h_\xi h_\omega W_{e_1}} \qquad (66)$$

After noting that both of these quanitities have bounded values, we find for the ω-momentum equation, Eq. (52),

$$\sigma G_{\eta\eta} - (V-\sigma H_m+\sigma_\eta)G_\eta + \frac{\sigma}{h_\omega}\left(\frac{h_{\xi,\eta}h_{\omega,\eta}}{h_\xi} - \frac{h_{\omega,\eta}^2}{h_\omega} + h_{\omega,\eta\eta}\right)G$$

$$- \frac{h_{\xi,0}\xi F}{2h_\xi^2}\, G_\xi = -\frac{1}{2}\left(\frac{h_{\xi,0}}{h_\xi}\right)^2 (1-FG)\beta_5$$

$$- \frac{1}{2}\left(\frac{h_{\omega,0}}{h_\omega}\right)^2 (1-G^2)\,\bar{\alpha}_1\beta_6 + \frac{\xi}{2}\left(\frac{h_{\omega,0}}{h_\omega}\right)^{-1}$$

$$\times \left(\frac{h_{\xi,0}}{h_\xi}\right)^2 (1-F^2)\,\frac{K_\xi}{\bar{\alpha}_2} - \frac{\xi A}{2h_{\omega,0}U_eW_e}\,\eta_{\bar{\omega}}$$

$$+ \frac{\xi}{2h_{\omega,0}U_eW_e}\,\frac{\partial}{\partial\omega}(I_\xi + I_\omega) \qquad (67)$$

Now, at the windward streamline,

$$\frac{\partial\eta}{\partial\bar{\omega}} = \frac{\eta}{2U_e}\,\frac{\partial U_e}{\partial\omega}$$

Thus,

$$\frac{\eta_{\bar{\omega}}}{W_e} = \sqrt{\frac{2}{U_e\xi}}\,\frac{U_{e_2}}{W_{e_1}} \qquad (68)$$

We also note that

$$I_\xi = U_e^2\sqrt{\frac{\xi}{2U_e}}\int_\eta^\infty \left(\frac{h_{\xi,0}}{h_\xi}\right)^3 (1-F^2)\,d\eta' \qquad (69)$$

$$I_\omega = W_e^2\sqrt{\frac{\xi}{2U_e}}\int_\eta^\infty \left(\frac{h_{\omega,0}}{h_\omega}\right)^3 (\bar{\alpha}_3^2 - G^2)\,d\eta' \qquad (70)$$

so that

$$\frac{1}{W_e}\frac{\partial I_\omega}{\partial \omega} = W_{e_1}\sqrt{\frac{\xi}{2U_e}}\int_\eta^\infty \left(\frac{h_{\omega,0}}{h_\omega}\right)^3 (\bar{\alpha}_3^2 - G^2)\,d\eta' \tag{71}$$

$$\frac{1}{W_e}\frac{\partial I_\xi}{\partial \omega} = \frac{2U_e U_{e_2}}{W_{e_1}}\sqrt{\frac{\xi}{2U_e}}\int_\eta^\infty \left(\frac{h_{\xi,0}}{h_\xi}\right)^3 (1-F^2)\,d\eta' \tag{72}$$

These latter results allow us to evaluate the last term in the ω-momentum equation.

Finally, we write for the symmetry plane energy equation

$$Pr^{-1}\,\theta_{\eta\eta} - (V+H_\theta)\theta_\eta - \frac{h_{\xi,0}\xi F}{h_\xi^2}\theta_\xi = -h_{\xi,0}^2\,\lambda\,F_\eta^2$$

$$+ \frac{4h_{\xi,0}\lambda}{h_\xi^4}\,h_{\xi,\eta}^2 \tag{73}$$

We also note that at locations where $\frac{\partial W_e}{\partial \omega} = 0$ the limit (57) is unbounded. From Eq. (63) we also see the term requiring G is not required and hence we do not need to solve the ω-momentum equation. Also note that $\frac{w}{W_e}\frac{\partial W_e}{\partial \omega} = w$ and hence the product $G\frac{\partial W_e}{\partial \omega}$ is bounded at the symmetry plane when $\frac{\partial W_e}{\partial \omega} = 0$.

6. Transformed Equations at the Stagnation Point

At the stagnation point, the properties at the edge of the boundary layer and the metrics at the surface are

$$\left.\begin{aligned} U_e &= U_1 \xi + \ldots \\ W_e &= W_1 \xi + W_2 \xi^2 + \ldots \\ h_\xi &= H_{1\xi} + H_{2\xi} \xi + \ldots \\ h_\omega &= H_{1\omega} \xi \end{aligned}\right\} \tag{74}$$

Let us first substitute the above relations into the inviscid irrotationality condition. This gives

$$\frac{1}{W_1} \frac{\partial U_1}{\partial \omega} = 2H_{1\omega,0}$$

At the stagnation point we take $W = W_e$ and write

$$\bar{\alpha}_1 = \bar{\alpha}_2 = \frac{W_1}{U_1} = \bar{\alpha} \tag{75a}$$

$$\bar{\alpha}_3 = 1 \tag{75b}$$

$$\beta_1 = 1 \tag{75c}$$

$$\beta_2 = 2\bar{\alpha} \tag{75d}$$

$$\beta_3 = \beta_5 = \begin{cases} 1 & W_1 \neq 0 \\ 2 & W_1 = 0 \end{cases} \tag{75e}$$

$$\beta_4 = \beta_6 = \begin{cases} \dfrac{1}{H_{1\omega,0} W_1} \dfrac{\partial W_1}{\partial \omega} & W_1 \neq 0 \\ \dfrac{1}{H_{1\omega,0} W_2} \dfrac{\partial W_2}{\partial \omega} & W_1 = 0 \end{cases} \tag{75f}$$

$$\xi K_{\xi,0} = \frac{1}{H_{1\omega,0}} \frac{\partial H_{2\xi,0}}{\partial \omega} \tag{75g}$$

$$K_{\omega,0} = \frac{1}{\xi} \tag{75h}$$

We now substitute these results into the continuity equation, Eq. (42)

$$V_\eta = -\frac{1}{H_{1\xi} H_{1\omega}} \sqrt{\frac{1}{2U_1}} \left[\frac{\partial}{\partial \xi} \left(\frac{2 H_{1\omega} H_{1\xi,0}}{H_{1\xi}} \sqrt{\frac{1}{2U_1}} \; U_1 F \right) \right.$$

$$\left. + \frac{\partial}{\partial \omega} \left(\frac{H_{1\xi} H_{1\omega,0}}{H_{1\omega}} \sqrt{\frac{1}{2U_1}} \; W_1 G \right) - H_{1\xi} \, H_{1\omega} \, V \frac{\partial (H_{1\xi} H_{1\omega})^{-1}}{\partial \eta} \right]$$

Thus,

$$V_\eta = -\frac{H_{1\xi,0}}{H_{1\xi}^2} F - \frac{H_{1\omega,0}\bar{\alpha}}{2H_{1\omega}} \frac{\partial G}{\partial \omega} + \left(\frac{\beta_4}{2} + \frac{\bar{\alpha}}{2}\right)\left(\frac{H_{1\omega,0}}{H_{1\omega}}\right)^2 \bar{\alpha} G$$

$$- \frac{H_{1\omega,0}\bar{\alpha}}{2H_{1\omega}^2}\left[\frac{1}{2H_{1\xi}} \frac{\partial H_{1\xi}}{\partial \omega} + \frac{1}{H_{1\omega,0}} \frac{\partial H_{1\omega,0}}{\partial \omega}\right.$$

$$\left. - \frac{1}{H_{1\omega}} \frac{\partial H_{1\omega}}{\partial \omega}\right] G + \left(\frac{1}{H_{1\omega}} \frac{\partial H_{1\omega}}{\partial \eta} + \frac{1}{H_{1\xi}} \frac{\partial H_{1\xi}}{\partial \eta}\right) V \quad (76)$$

Before the ξ-momentum equation is evaluated note

$$\xi L_\xi = 0$$

$$\frac{\xi \eta_\xi}{U_e^2} = \frac{\xi}{U_1^2 \xi^2} \frac{\partial}{\partial \xi} \sqrt{2U_1}\ \bar{n} = 0$$

$$\frac{\xi}{U_e^2} \frac{\partial I_\xi}{\partial \xi} = \frac{\sqrt{2}\ I_{1\xi}}{U_1^2}\ ;\quad I_{1\xi} = \int_\eta^\infty \left(\frac{h_{\xi,0}}{h_\xi}\right)^3 (1-F^2)\, d\eta'$$

$$\frac{\xi}{U_e^2} \frac{\partial I_\omega}{\partial \xi} = \frac{\sqrt{2}\ W_1^2 I_{1\omega}}{U_1^{3/2}}\ ;\ I_{1\omega} = \int_\eta^\infty \left(\frac{H_{1\omega,0}}{H_{1\omega}}\right)^3 (1-G^2)\, d\eta'$$

Using these results, Eq. (44), the ξ-momentum equation, becomes

$$\sigma F_{\eta\eta} - (V + \sigma H_m + \sigma_\eta) F_\eta - \left[+ \sigma \left(\frac{h_{\omega,\eta} h_{\xi,\eta}}{h_\xi h_\omega} - \frac{h_{\xi,\eta}^2}{h_\xi^2} + \frac{h_{\xi,\eta\eta}}{h_\xi} \right) - \sigma_\eta \frac{h_{\xi,\eta}}{h_\xi} \right] F$$

$$- \frac{H_{1\omega,0} G\bar{\alpha}}{2H_{1\omega}^2} F_\omega = - \frac{1}{2} \left(\frac{h_{\xi,0}}{h_\xi} \right)^2 (1-F^2) - \frac{\bar{\alpha}}{2} \left(\frac{H_{1\omega,0}}{H_{1\omega}} \right)^2$$

$$\times \ (2\bar{\alpha} - \xi K_{\xi,0}) \ (1-FG) - \frac{\bar{\alpha}^2}{2} \left(\frac{h_{\xi,0}}{h_\xi} \right)^{-1} \left(\frac{H_{1\omega,0}}{H_{1\omega}} \right)^2$$

$$\times \ (1-G)^2 + \frac{\sqrt{2}}{U^2} \left[I_{1\xi} + \frac{W_1^2 \, I_{1\omega}}{U} \right] \qquad (77)$$

Before the ω-momentum equation is evaluated note

$$\frac{\beta_2}{\bar{\alpha}} = \frac{2\bar{\alpha}}{\bar{\alpha}} = 2$$

$$\bar{\alpha}\beta_6 = \bar{\alpha}\beta_4 = \frac{1}{H_{1\omega,0} U_1} \frac{\partial W_1}{\partial \omega} \qquad W_1 \neq 0$$

$$= \frac{\bar{\alpha}}{H_{1\omega,0} W_2} \frac{\partial W_2}{\partial \omega} = 0 \qquad W_0 = 0$$

$$\frac{\xi K_\xi}{\bar{\alpha}} = \frac{U_1}{H_{1\xi} H_{1\omega} W_1} \frac{\partial H_{1\xi}}{\partial \omega} \qquad W_1 \neq 0$$

$$= \frac{U_1}{W_2} \frac{1}{H_{1\xi} H_{1\omega}} \frac{\partial H_{2\xi}}{\partial \omega} \qquad W_1 = 0$$

Define

$$A_1 = -\frac{\sqrt{2}}{2} \left[- \frac{h_{\xi,0}^2 U_1^2 (1-F^2)}{h_\xi^2} \frac{\partial H_{1\xi}}{\partial \eta} - \left(\frac{h_{\xi,0}}{h_\xi} \right)^3 \sqrt{\frac{U_1^3}{2}} (1-F^2) \right.$$

$$\left. - \frac{W_1}{\sqrt{2U_1}} (1-G^2) - \frac{H_{1\omega,0}^2 W_1^2 (1-G^2)}{H_{1\omega}^3} \frac{\partial H_{1\omega}}{\partial \eta} \right]$$

giving

$$\frac{\xi A \eta_\omega}{2 h_{\omega,0} U_e W} = \frac{A_1}{U_1^{3/2}} \bar{\eta_\omega}$$

also,

$$\frac{\xi}{2 h_{\omega,0} U_e W} \frac{\partial I_\xi}{\partial \omega} = \frac{3}{\sqrt{2U_1}} I_{1\xi} + \frac{\sqrt{U_1}}{\sqrt{2}\, H_{1\omega,0} W_1} \frac{\partial I_{1\xi}}{\partial \omega}$$

and

$$\frac{\xi}{2 h_{\omega,0} U_e W} \frac{\partial I_\omega}{\partial \omega} = \frac{I_{1\omega}}{\sqrt{2}\, H_{1\omega,0} U_1^{3/2}} \frac{\partial W_1}{\partial \omega} - \frac{\bar{\alpha}^2 I_{1\omega}}{\sqrt{2}\, U_1^{1/2}} \frac{\partial U_1}{\partial \omega}$$

$$+ \frac{\bar{\alpha}}{\sqrt{2}\, H_{1\omega,0} U_1^{1/2}} \frac{\partial I_{1\omega}}{\partial \omega}$$

With these results the ω-momentum equation, Eq. (52) becomes

$$\sigma G_{\eta\eta} - (V - \sigma H_m + \sigma_\eta) G_\eta - \left[\sigma \left(\frac{h_{\xi,\eta} h_{\omega,\eta}}{h_\xi h_\omega} - \frac{h_{\omega,\eta}^2}{h_\omega} + \frac{h_{\omega,\eta\eta}}{h_\omega} \right) - \sigma_\eta \frac{h_{\omega,\eta}}{h_\omega} \right] G - \frac{\bar{\alpha} H_{1\omega,0}}{2H_{1\omega}^2} G G_\omega = - \left(\frac{h_{\xi,0}}{h_\xi} \right)^2 (1-FG) \frac{\beta_5}{2}$$

$$- \frac{\bar{\alpha}}{2} \left(\frac{H_{1\omega,0}}{H_{1\omega}} \right)^2 (1-G^2) \beta_6 + \left(\frac{H_{1\omega,0}}{H_{1\omega}} \right)^{-1} \left(\frac{h_{\xi,0}}{h_\xi} \right)^2$$

$$(1-F^2) \frac{\xi K_\xi}{2\alpha} - \frac{1}{2} \left(\frac{h_{\xi,0}}{h_\xi} \right)^2 (1-FG) - \frac{A_1}{U_1^{3/2}} + \frac{3}{\sqrt{2U_1}} I_{1\xi}$$

$$+ \frac{\sqrt{U_1}}{\sqrt{2}\, H_{1\omega,0} W_1} \frac{\partial I_{1\xi}}{\partial \omega} + \left[\frac{2}{W_{\omega,0} U_2} \frac{\partial W_1}{\partial \omega} - \bar{\alpha}^2 \right]$$

$$\frac{I_{1\omega}}{\sqrt{2U_1}} + \frac{\bar{\alpha}}{\sqrt{2}\, H_{1\omega,0} U_1^{1/2}} \frac{\partial I_{1\omega}}{\partial \omega} \tag{78}$$

Finally, the energy equation becomes

$$Pr^{-1} \theta_{\eta\eta} - (V + H_\theta) \theta_\eta + \frac{\bar{\alpha} G}{2H_{1\omega}} \theta_\omega = - \lambda F_\eta^2$$

$$+ \frac{4h_{\xi,0}\lambda}{h_\xi^4} h_{\xi,\eta}^2 + \frac{4\lambda^2 \bar{\alpha}^2}{H_{1\omega}^2} \left(\frac{\partial H_{1\omega}}{\partial \eta} \right)^2 \tag{79}$$

7. Coordinate System and Metric Coefficients

The orthogonal surface curvilinear coordinate system used to write the boundary-layer equations is identical to the one developed by Blottner and Ellis (Ref. 2). As shown in Fig. 1 the three coordinate directions are ξ, ω, n. For each set of ξ, ω, n there corresponds a set x, θ, r in the polar coordinate system whose origin is at the stagnation point. The inviscid data tape contains data in the ξ, ω, n coordinate system and at each point the corresponding values of x, θ, r are written. The transformation between the two coordinate systems is generated numerically in program BLOT which is contained in the TAPGEN program (see Ref. 7). The procedure is identical to that of Ref. 2. For each point in the ξ, ω, n system, program BLOT also generates values of $h_{\xi,0}$ and $h_{\omega,0}$ and these quantities, along with their ξ-derivatives are also written on the inviscid data tape.

The boundary-layer program itself contains routines to generate values of h_ξ and h_ω as functions of n for points in the boundary layer away from the wall. These routines are used only in calculations where surface curvature effects are included. For cases where no surface curvature effects are included, the following relations are used:

$$\left.\begin{aligned} h_\xi &= h_{\xi,0} \\ h_\omega &= h_{\omega,0} \\ h_{\xi,\eta} &= h_{\xi,\eta\eta} = 0 \\ h_{\omega,\eta} &= h_{\omega,\eta\eta} = 0 \end{aligned}\right\} \qquad (80)$$

In order to calculate the values of the metric coefficients away from the wall the definitions of the metrics are used, i.e.

$$h_\xi^2 = \frac{ds^2}{d\xi^2} = \frac{dx^2 + dr^2 + (rd\phi)^2}{d\xi^2} \tag{81}$$

$$h_\omega^2 = \frac{dt^2}{d\omega^2} = \frac{dx^2 + dr^2 + (rd\phi)^2}{d\omega^2} \tag{82}$$

where s and t are defined in Fig. 2 . The following definitions are now made,

$$\left.\begin{aligned} x &= x_0 + \tilde{x} \\ r &= r_0 + \tilde{r} \\ \phi &= \phi_0 + \tilde{\phi} \end{aligned}\right\} \tag{83}$$

Thus,

$$h_\xi^2 = \frac{dx_0^2 + dr_0^2}{d\xi^2} + \frac{2d\tilde{r}\ dr_0 + d\tilde{r}^2}{d\xi^2} + \frac{[(r_0+\tilde{r})(d\phi_0+d\tilde{\phi})]^2}{d\xi^2}$$

$$+ \frac{2d\tilde{x}dx + d\tilde{x}^2}{d\xi^2} = h_{\xi,0}^2 + \tilde{h}_\xi \tag{84}$$

and

$$h_\omega^2 = \frac{dx_0^2 + dr_0^2 + r_0^2\, d\phi_0^2}{d\omega^2} + \frac{2d\tilde{r}\ dr_0 + d\tilde{r}^2}{d\omega^2}$$

$$+ \frac{(r_0 d\tilde{\phi})^2 + \tilde{r}^2\ (d\phi_0 + d\tilde{\phi})^2}{d\omega^2} + \frac{2d\tilde{x}\ dx_0 + d\tilde{x}^2}{d\omega^2}$$

$$= h_{\omega,0}^2 + \tilde{h}_\omega \tag{85}$$

The above expressions are evaluated numerically using the values of $\tilde{x}$, $\tilde{r}$, and $\tilde{\phi}$ for points in the profiles. If g is taken to represent $\tilde{x}$, $\tilde{r}$ or $\tilde{\phi}$ then (see Fig. 3).

$$\left(\frac{dg}{d\xi}\right)_{2,n} = \frac{g_{2,n} - g_{3,n}}{\xi_2 - \xi_3} \tag{86}$$

$$\left(\frac{dg}{d\omega}\right)_{2,n} = \frac{g_{2,n} - g_{1,n}}{\omega_2 - \omega_1} \tag{87}$$

The positions of the coordinates themselves are generated with the numerical scheme of Blottner and Ellis (Ref. 2). This procedure is first-order accurate and requires relatively small step sizes in ξ and ω. For this reason the coordinate generation routine was coded independently of the boundary-layer program so that the coordinate system could be generated on the fine mesh and the boundary-layer equations evaluated over a coarser mesh.

8. Eddy Viscosity Models

Prandtl's mixing length hypothesis states that the eddy viscosity is the product of some characteristic length and the normal velocity gradient. The characteristic length is related to the size of the eddies of momentum flux normal to the body and is called the mixing length. For two-dimensional flow this concept leads to:

$$\varepsilon = \rho \ell_*^2 \left| \partial u / \partial n \right| \tag{88}$$

Prandtl's studies assumed that the eddy viscosity should depend only on local eddy scale and on the properties of turbulence. Adams (Ref. 8) extended this concept to the three-dimensional case by assuming that the eddy viscosity is also independent of coordinate direction by writing the component of turbulent stress terms as:

$$\tau_{t_\xi} = -\rho u'v' = \rho \ell_*^2 \, \partial E/\partial n \;\; \partial u/\partial n \tag{89}$$

$$\tau_{t_\omega} = -\rho v'w' = \rho \ell_*^2 \, \partial E/\partial n \;\; \partial u/\partial n \tag{90}$$

where E is some scalar function. Therefore,

$$\varepsilon = \varepsilon_\xi = \varepsilon_\omega = \rho \ell_*^2 \;\; \partial E/\partial n \tag{91}$$

The total shear in each direction is written as:

$$\tau_\xi = \mu \, \partial u/\partial n - \rho u'v' = \mu \, \partial u/\partial n + \varepsilon_\xi \, \partial u/\partial n \tag{92}$$

$$\tau_\omega = \mu \, \partial w/\partial n - \rho w'v' = \mu \, \partial w/\partial n + \varepsilon_\omega \, \partial w/\partial n \tag{93}$$

therefore the total resultant shear is written as:

$$\tau = \left[\tau_\xi^2 + \tau_\omega^2\right]^{1/2} = \left[(\mu + \varepsilon_\xi)^2 \, (\partial u/\partial n)^2 + (\mu + \varepsilon_\omega)^2 (\partial w/\partial n)^2\right]^{1/2} \tag{94}$$

Using equations (94) and (91) the total resultant shear becomes:

$$\tau = \left[\mu + \rho \ell_*^2 \;\; \partial E/\partial n\right] \left[(\partial u/\partial n)^2 + (\partial w/\partial n)^2\right]^{1/2} \tag{95}$$

By analogy with the two-dimensional case where the eddy viscosity expression incorporates the velocity gradient of the shear component, the scalar E becomes:

$$\partial E/\partial n = \left[(\partial u/\partial n)^2 + (\partial w/\partial n)^2\right]^{1/2} \tag{96}$$

$$\varepsilon = \varepsilon_\xi = \varepsilon_\omega = \rho \ell_*^2 \left[(\partial u/\partial n)^2 + (\partial w/\partial n)^2\right]^{1/2} \tag{97}$$

which reduces to the two-dimensional form when w = 0. This is referred to as the invariant turbulence model by Hunt, Bushnell, and Beckwith (Ref. 9), and was used with success by Adams (Ref. 8).

The model used in this investigation is the common two-layer inner-outer model which uses the Prandtl mixing length theory and the Van Driest or Reichardt damping near the wall. Following Patankar and Spalding (Ref. 10) and Adams (Ref. 8) the mixing length distribution is as follows:

$$\ell_* = k_* \, n \qquad \{0 < n \geq \lambda n_\ell / k_*\}$$

$$\ell_* = \lambda \cdot n_\ell \qquad \{\lambda n_\ell / k_* < n\} \tag{98}$$

where

$$k_* = 0.435$$

$$\lambda = 0.09$$

$$n_\ell = n \text{ when } \left[(u^2 + w^2)/(U_e^2 + W_e^2)\right]^{1/2} = 0.99$$

The inner law is damped near the wall so as to yield the exact laminar shear stress term at the wall. To accomplish this, two different damping factors have been used in this investigation,

Van Driest's damping term with local shear stress, and Reichardt's (Ref.11) damping term.

Van Driest's damping term for two-dimensional flow is:

$$\ell_{*_i} = 1 - \exp\left(\frac{-n\sqrt{\tau\rho}}{\mu A^*}\right) \tag{99}$$

where τ is the local shear stress and A^* is 26.0. Therefore the total shear near the wall becomes:

$$\tau = \mu\, \partial u/\partial n + \rho k_*^2\, n^2 \left[1 - \exp\left(\frac{-n\sqrt{\tau\rho}}{\mu A^*}\right)\right]^2 (\partial u/\partial n)^2 \tag{100}$$

for two-dimensional flow. Again, use is made of analogy to derive the form of the near wall shear for a three-dimensional flow. By analogy of equation (100) with equations (95) and (96) the three-dimensional form of the total shear becomes:

$$\tau_i = \mu\, \partial E/\partial n + \rho k_*^2\, n^2 \left[1 - \exp\left(\frac{-n\sqrt{\tau\rho}}{\mu A^*}\right)\right]^2 (\partial E/\partial n)^2 \tag{101}$$

or

$$\varepsilon_i = \rho k_*^2\, n^2 \left[1 - \exp\left(\frac{-n\sqrt{\tau\rho}}{\mu A^*}\right)\right]^2 (\partial E/\partial n) \tag{102}$$

Cebeci (Ref. 12) developed a mass-transfer correction to Van Driest's inner eddy viscosity law by modifying the damping constant A^*. For turbulent flows with mass transfer Cebeci determined the damping constant to be

$$A^* = 26 \exp(-5.9\, v_0^+)$$

where

$$v_0^+ = v_0/(\tau_0/\rho)^{1/2}$$

Reichardt's expression for the inner eddy viscosity law was obtained by curve fitting experimental pipe flow data. The expression is:

$$\varepsilon_i = \mu k_* \left[\frac{n\sqrt{\tau\rho}}{\mu} - 11.0 \tanh \left(\frac{n\sqrt{\tau\rho}}{11\mu} \right) \right] \qquad (103)$$

As can be seen this expression does not involve the velocity gradient terms. For this reason it is preferred for use in numerical solutions, since it usually requires fewer iterations to converge.

Following equations (97) and (98) the outer eddy viscosity law is:

$$\varepsilon_0 = \lambda^2 n_\ell^2 \, \partial E/\partial n \qquad (104)$$

and the total shear stress is:

$$\tau_0 = \mu \, \partial E/\partial n + \lambda^2 n_\ell^2 \, (\partial E/\partial n)^2 \qquad (105)$$

The outer eddy viscosity law is used in conjunction with the Klebanoff (Ref. 13) intermittency factor which assures a smooth approach of ε_0 to zero as $y \to \delta$. The modified law is:

$$\varepsilon_0 = \lambda^2 n_\ell^2 \, \gamma \, \partial E/\partial n \qquad (106)$$

where γ is Klebanoff's intermittency factor:

$$\gamma = \left[1 + 5.5 \, (n/\delta)^6 \right]^{-1} \qquad (107)$$

Schetz and Favin (Ref.14) have derived a correction to Reichardt's inner eddy viscosity law for cases of mass transfer. This correction has been used in the current investigation, giving this corrected expression for the inner eddy viscosity:

$$\varepsilon_i = k\mu\ (1 + v_0^+\ u^+)^{1/2}\ (n^+ - n_e^+ \tanh\ (n^+/n_e^+)) \quad (108)$$

where

$$v_0^+ = v_0/\sqrt{\tau_0/\rho}$$

$$n^+ = n\sqrt{\tau\rho/\mu}$$

and

$$n_e^+ = 3.65/(v_0^+ + 0.344)$$

The quantity u^+ is found by integration of the expression

$$\frac{du^+}{dn^+} = \frac{(1 + v_0^+\ u^+)}{1 + k\ (1 + v_0^+\ u^+)^{1/2}\ (n^+ - n_e^+ \tanh\ (n^+/n_e^+))} \quad (109)$$

or using equation (108):

$$\frac{du^+}{dn^+} = \frac{(1 + v_0^+\ u^+)}{(1 + \varepsilon_i)} \quad (110)$$

Since the eddy viscosity ε_i is implicit in the integration for u^+, the calculation of ε_i is an iterative procedure for mass transfer cases.

9. Transition Models

Two models of transition from laminar to turbulent flow have been used in this investigation. One model is a simply instantaneous transition to turbulent flow, and there really is no transition region or zone at all. In the second case a smooth transition to turbulent flow occurs over a prescribed distance. This distance is known as the transition zone and is defined as the distance between the onset of transition at $\xi = \xi_t$ and the beginning of fully turbulent flow at $\xi = \xi_T$ at some point downstream.

The probability of turbulent flow at any point is expressed by a model by Dhawan and Narasimha (Ref. 15) as:

$$I_f(\xi) = 1 - \exp\left(-\Phi\left((X-X_t)/\bar{\chi}\right)^2\right) \tag{111}$$

where $I_f(x)$ is the transition intermittency factor, and

$$\Phi = 0.412$$

$$\bar{\chi} = X_{I_f = 0.75} - X_{I_f = 0.25}$$

and where

$$\left.\begin{aligned} I_f(X_t) &= 0 \\ I_f(X_T) &= 0.97 \end{aligned}\right\} \tag{112}$$

By substituting equation (112) into (111) an expression for $\bar{\chi}$ can be found based on the transition zone length:

$$\bar{\chi} = (X_T - X_t)/2.917 \tag{113}$$

Now, substituting (113) back into (111) the final expression for the transition intermittency factor as used in this investigation is obtained:

$$I_f(\xi) = 1 - \exp\left[\, 0.412\ (2.917)^2\ ((X-X_t)/(X_T-X_t))^2 \,\right] \quad (114)$$

The transition intermittency factor is employed as a simple multiplier of the eddy viscosity in the governing equations and therefore acts as a damping coefficient for the full turtulent eddy viscosity. It is an expression relating the fraction of time any particular point spends in turbulent flow, and therefore the probability of turbulent flow existing at that point.

10. Finite-Difference Method

The finite difference method used in this investigation is idential to the one used by Frieders and Lewis (Ref.17). Basically the procedure is based on the method of Dwyer (Ref.18) with modifications by Krause (Ref.19). The procedure allows for variable spacing of the normal coordinate.

As implemented in the current investigation, the finite-difference procedure is a forward marching one, thus taking advantage of the parabolic nature of the governing equations. The method used marches away from the stagnation point by first stepping down the windward symmetry plane one step and then marching around the body from the windward to leeward symmetry plane. This process is repeated until the calculation is completed.

Basically the finite-difference procedure is implicit in the normal direction and explicit in the ξ- and ω-directions. In order to retain stability in regions of reversed cross-flow, the Krause difference molecule is used for ω differencing as depicted in Fig. 3 . Taking w to be a general variable (i.e. either F, G or θ) then

$$\frac{\partial w}{\partial \xi} = \frac{w_{2,n} - w_{3,n}}{\Delta \xi}$$

$$\frac{\partial w}{\partial \omega} = \frac{(w_{2,n} - w_{1,n}) + (w_{4,n} - w_{3,n})}{2\Delta \omega}$$

where the subscript notation is that of Fig. 3 . Central differences are used in the normal direction with mesh points spaced according to the formula

$$k = \frac{\Delta\eta_n}{\Delta\eta_{n-1}}$$

where k is a constant which can be set at the discretion of the user. Substitution of the finite-difference expressions into the governing equations results in a set of non-linear difference equations of the form

$$-\tilde{A}_n w_{2,n-1} + \tilde{B}_n w_{2,n} - \tilde{C}_n w_{2,n+1} + \tilde{E}_n w^2_{2,n} = \tilde{D}_n \qquad (115)$$

This relation is linearized using the Newton-Raphson interation formula

$$w^2_{2,n} = 2w^0_{2,n}\, w_{2,n} - (w^0_{2,n})^2 \qquad (116)$$

where $w^0_{2,n}$ is the value of the dependent variable from the previous iteration. For the initial iteration, $w^0_{2,n}$ is approximated with $w_{1,n}$. Use of Eq.(116) in Eq.(115) results in a set of simultaneous linear algebraic equations of the form

$$-A_n w_{2,n-1} + B_n w_{2,n} + C_n w_{2,n+1} = D_n$$

which are solved using the Thomas algorithm (Ref. 20).

11. Normal Pressure Gradient Approximation

The normal pressure gradient which appears in the normal momentum equation, Eq. (14) basically arises from centrifugal force effects. Due to the low speeds being considered in the current work this effect was neglected.

This was done by setting I_ξ and I_ω to zero in Eqs. (44) and (52). In the actual coding however these terms were left in the governing equations and this effect could easily be included in the future by having subroutine PRESSI evaluate Eqs. (45) and (46) in program ICBL3D.

Section III

RESULTS AND DISCUSSION

In order to test the validity and accuracy of the computer program developed from the foregoing analysis, a variety of test cases was selected. Since the principle departure of the present analysis from previous efforts is in the inclusion of surface curvature effects, it was this area that received considerable attention during the testing process. Test cases were run at a Reynolds number of one hundred in order to achieve a thick boundary layer on the body, thus amplifying the curvature effects. Calculations were made over spheres and spheroids at various angles of attack and turbulent effects were included in one comparison.

The first test case run was that of a sphere at angle of attack. In this calculation a coordinate system is selected that is not aligned with the sphere's wind axis thus producing the requirement for a three-dimensional calculation of the body boundary layer. The utility of this calculation is that it can be easily compared with existing axisymmetric boundary-layer calculations. Calculations were made for a unit sphere at $\alpha = 2^{o}$, $Re_{\infty} = 100$. The results were compared with those of Davis et al. (Ref. 6). The results of Ref. 6 were obtained with an axisymmetric boundary-layer code with longitudinal and transverse curvature effects included (SFC). The results of these comparisons are shown in Figs. 4 through 6. Plotted in Fig. 4 is the development of the skin friction and displacement thickness

along the windward symmetry plane of the sphere. The results of the present calculation without surface curvature (NoSFC) agree identically with predictions made by the VPI&SU axisymmetric boundary-layer code (Ref. 16). The skin-friction comparison between the present method and that of Davis et al. (Ref. 6) for the SFC case is also excellent. Figure 5 shows the variation of skin friction around the sphere along ξ=constant lines. Compared in Fig. 6 are the velocity profiles at a point on the windward symmetry plane for the with and without SFC cases.

Calculations were then made over a 4:1 spheroid at $\alpha = 2^{o}$ and $Re_{\infty} = 100$. The semi-major axis of the body was aligned with the angle of attack line and was four feet long. The results of these calculations are shown in Figs. 7 through 10. Figure 7 illustrates the development of the boundary layer along the windward symmetry plane. The skin friction for the No SFC case is compared with an unpublished calculation made with the Blottner and Ellis (Ref. 2) code. As can be seen the agreement is excellent. Figure 8 illustrates the development of the skin friction around the body and compares the results with that of the Blottner and Ellis code for the NoSFC case. In Figs. 9 and 10 velocity profiles are compared between the two codes.

An interesting result of these calculations is that inclusion of surface curvature effects initially produces a somewhat thicker body boundary layer compared with the NoSFC case. This is in contrast to the inclusion of transverse curvature effects only which initially produces a thinner boundary

layer compared with the NoSFC case (see Ref. 6). Since the pressure gradients experienced by the boundary layer over flatter portions of the spheroidal body where longitudinal curvature effects become less important are not such as to thin the boundary layer, this thicker boundary-layer persists along the body. The results indicate that all curvature effects must be accounted for in order to correctly predict the boundary layer growth over blunt nosed bodies.

Figures 11 and 12 detail the boundary-layer growth for the same 4:1 spheroidal body at $\alpha = 10^{o}$. The effects of this larger angle of attack are clearly seen by comparing the circumferential skin friction plot of Fig. 12.

In Figure 13 a turbulent calculation is presented for a 4:1 spheroid at $\alpha = 0^{o}$ and $Re_{\infty} = 10^{7}$. Comparison is made between the present method and the results of Chang and Patel (Ref. 3). As can be seen the agreement is excellent.

These calculations were made to verify the code and as can be seen by the calculated results, agreement between the present method and previously published works is excellent. It should be borne in mind, however, that the present code is much more versatile than either the codes of Refs. 2 or 3 in that it includes surface curvature effects, it can treat arbitrary body shapes and it includes turbulence effects.

SECTION IV

CONCLUDING REMARKS

The total system of computer programs generated to implement the foregoing analysis represents a package with very general capabilities. These capabilities are as follows:

1. Body must have a blunt nose and a plane of symmetry but is otherwise arbitrary so far as the boundary-layer code is concerned at arbitrary angle of attack.
2. Current inviscid capabilities are restricted to axisymmetric shapes at zero and non-zero angles of attack and arbitrary cross-sections at zero angle of attack.
3. All surface curvature effects included.
4. Laminar, transitional and/or turbulent flows can be calculated.
5. Effects of heat and mass transfer included.

To the authors' knowledge these capabilities represent the most complete package available today for predicting three-dimensional boundary layers.

The system of programs was separated into two independent systems of programs in order to maximize operational versatility and to facilitate future development. By removing the calculation of the inviscid flow and coordinate system from the boundary-layer code, this boundary-layer code can be viewed as a solution procedure for the set of governing equations

developed in Section II. The separate inviscid flow computer program supplies data to this solver which defines both the body geometry and inviscid flow. Thus, if alternate means for generating either the inviscid flow or coordinate system are desired, other methods can be substituted into the appropriate blocks in the inviscid package without affecting the boundary-layer code. Further, the separate boundary-layer calculation is allowed to proceed on its' own step size along the surface without considering mesh requirements of the inviscid flow or coordinate generation codes.

In summary, the analysis and programs resulting from this investigation represent as versatile, flexible, general and efficient a method for predicting incompressible three-dimensional boundary-layers available today.

REFERENCES

1. Moore, F. K., "Three-Dimensional Boundary-Layer Theory," Advances in Applied Mechanics, Vol. 4, pp. 160-228, 1956.

2. Blottner, F. G. and Ellis, M., "Three-Dimensional, Incompressible Boundary Layer on Blunt Bodies. Part I: Analysis and Results," Sandia Laboratories Report No. SLA-73-0366, Albuquerque, New Mexico, April 1973.

3. Chang, K. C. and Patel, V. C., "Calculation of Three-Dimensional Boundary Layers on Ship Forms," Iowa Institute of Hydraulic Research Report No. IIHR 178, Iowa City, Iowa, June 1975.

4. Hess, J. L. and Martin, R. P., Jr., "Improved Solution for Potential Flow about Arbitrary Axisymmetric Bodies by the Use of a Higher-Order Surface Source Method: Part I. Theory and Results." NASA CR 134694, Cleveland, Ohio, July 1974.

5. Hughes, W. F. and Gaylord, E. W., Basic Equations of Engineering Science, Schaum Publishing Company, New York, 1964.

6. Davis, R. I., Whitehead, R. E. and Wornom, S. F., "The Development of an Incompressible Boundary-Layer Theory Valid to Second Order," Virginia Polytechnic Institute College of Engineering Report VPI-E-70-1, Blacksburg, Virginia, January 1970.

7. Dwoyer, D. L., Lewis, Clark H. and Gogineni, P. R., "Three-Dimensional Incompressible Boundary Layers on Blunt Bodies Including Effects of Turbulence, Surface Curvature and Heat and Mass Transfer. Part I: Analysis and Results." VPI&SU Aero-063, May 1977.

8. Adams, J. C., "Implicit Finite-Difference Analysis of Compressible Laminar, Transitional and Turbulent Boundary Layers along the Windward Streamline of a Sharp Cone at Incidence," AEDC-TR-71-235, December 1971.

9. Hunt, J. L., Bushnell, J. M. and Beckwith, I.E. "Finite Difference Analysis of the Compressible Turbulent Boundary Layer on a Blunt Swept Slab with Leading Edge Blowing," NASA TN D-6203, March 1971.

10. Patankar, S. V. and Spalding, D. B., Heat and Mass Transfer in Boundary Layers, CRC Press, Cleveland, Ohio, 1968.

11. Reichardt, H., "Vollstandige Darstellung der Turbulenten Geschwindig-keitsverteilung in glatten Lutungen," ZAMM 31, 1951, pp. 208-219.

12. Cebeci, T., "Behavior of Turbulent Flow Near a Porous Wall with Pressure Gradient," AIAA J., Vol. 8, No. 12, December 1970.

13. Klebanoff, P. S., "Characteristics of Turbulence in a Boundary Layer with Zero Pressure Gradient," NASA TN-3178, 1954.

14. Schetz, J. A. and Favin, S., "Numerical Calculation of Turbulent Boundary Layers Including Suction or Injection with Binary Diffusion," Astronautica Acta, Vol. 16, pp. 339-352, Pergamon Press, 1971.

15. Dhawan, S. and Narasimha, R., "Some Properties of Boundary Layer Flow during Transition from Laminar to Turbulent Motion," J. Fluid Mech., Vol. 3, No. 4, April 1958, pp. 418-426.

16. Dwoyer, D. L., Lewis, Clark H. and Frieders, M. C., "A Program for Laminar Transitional and/or Turbulent, Two-Dimensional or Axisymmetric Boundary Layers Including Effects of Transverse Curvature," VPI&SU Department of Aerospace and Ocean Engineering, Internal Memo, November 1975.

17. Frieders, M. C. and Lewis, C. H., "Effects of Mass Transfer into Laminar and Turbulent Boundary Layers over Cones at Angles of Attack," Report VPI-AERO-031, March 1975.

18. Dwyer, H. A., "Boundary Layer on a Hypersonic Sharp Cone at Small Angle of Attack," AIAA J., Vol. 9, No. 2, pp. 277-284, February 1971.

19. Krause, E., "Comment on 'Solution of a Three-Dimensional Boundary-Layer Flow with Separation'," AIAA J., Vol. 7, No. 3, March 1969.

20. Roache, P. J., Computational Fluid Dynamics, Hermosa Publishers, Albuquerque, New Mexico, 1972.

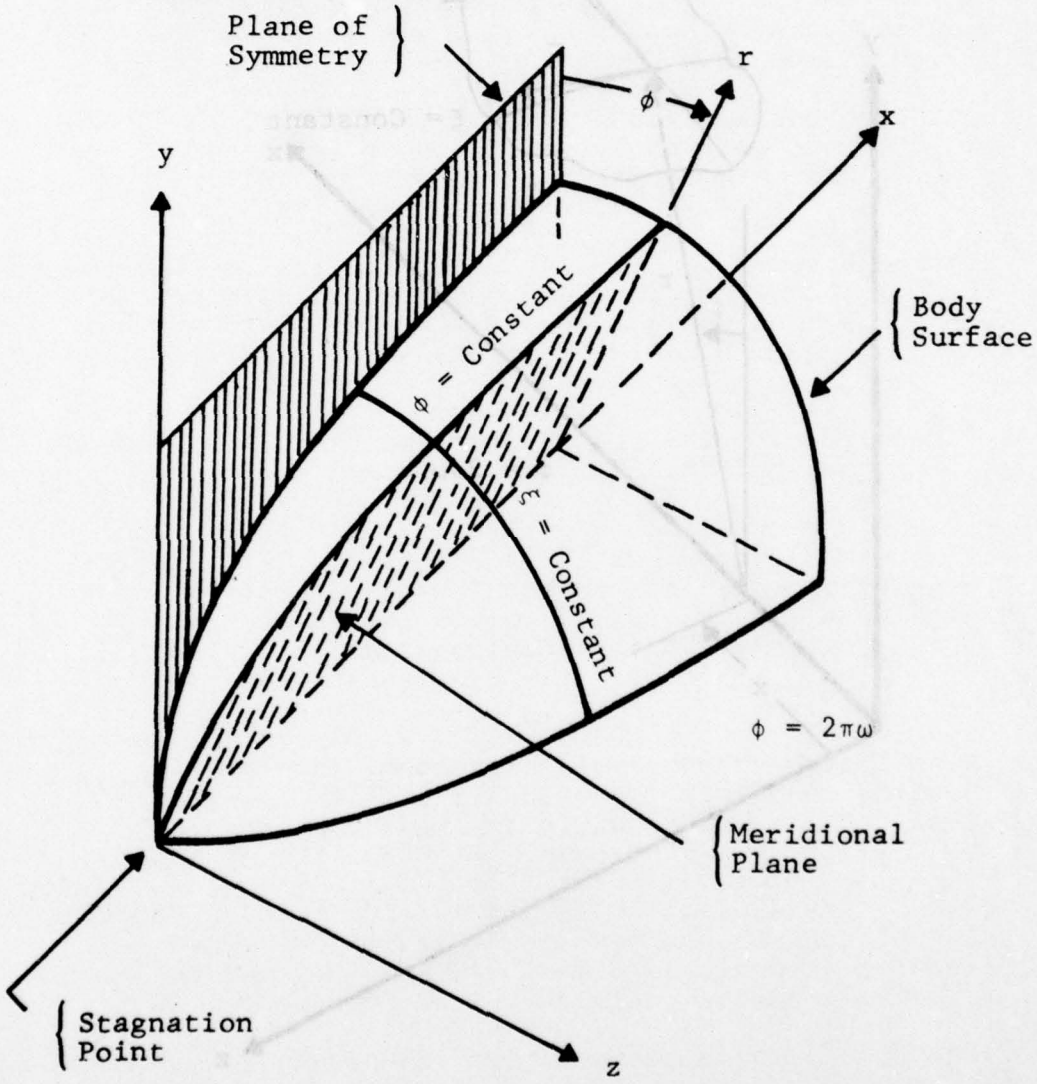

Figure 1. SURFACE COORDINATE SYSTEM

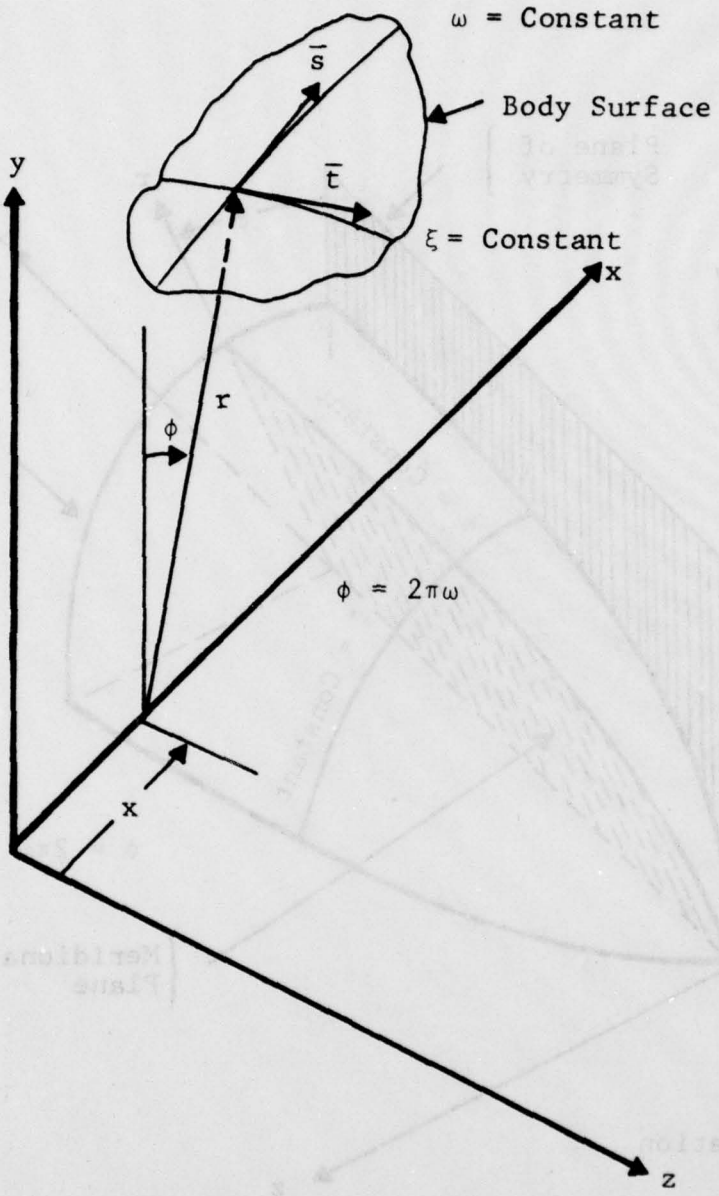

Figure 2. RELATION BETWEEN SURFACE COORDINATES

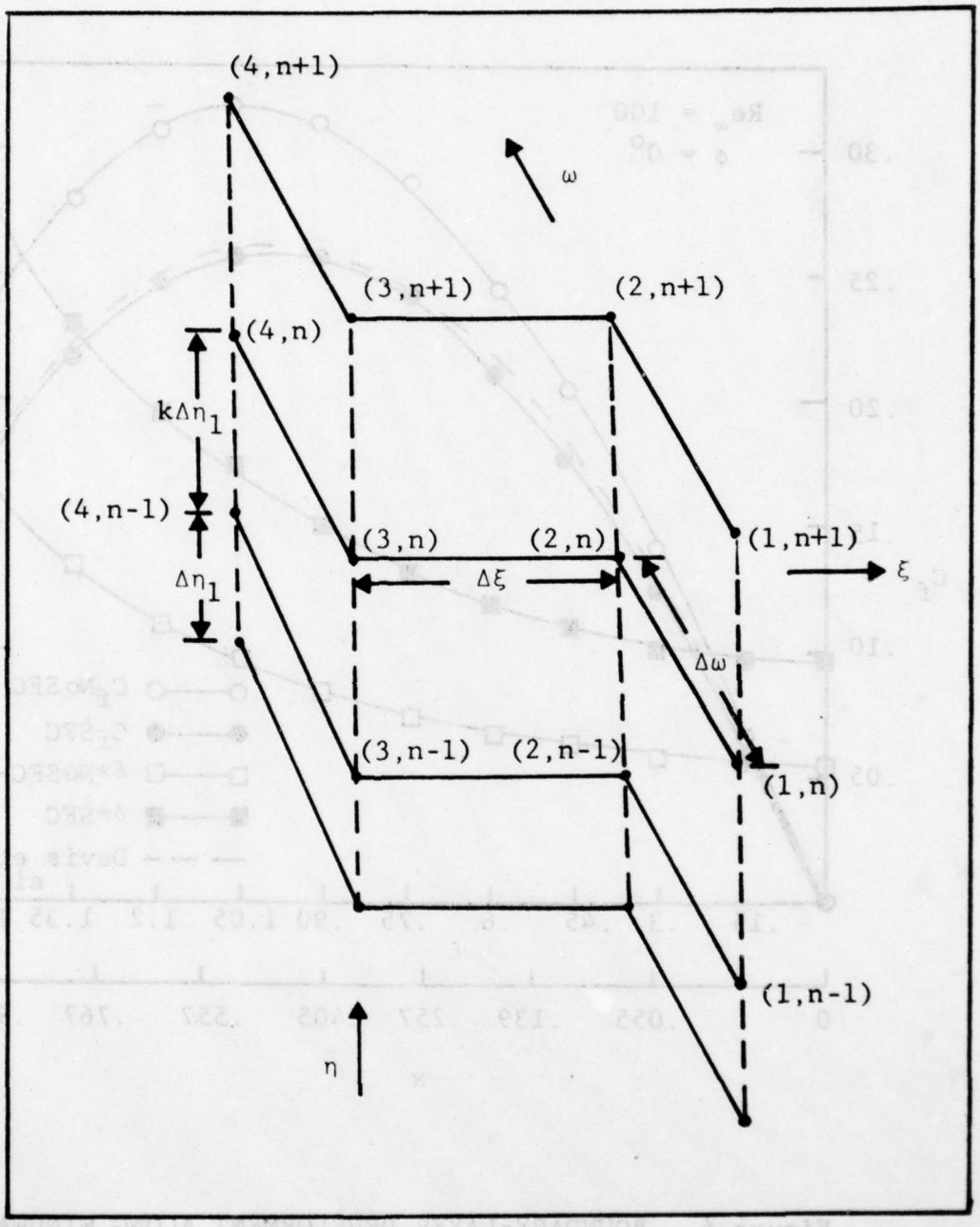

Figure 3. FINITE-DIFFERENCE MESH

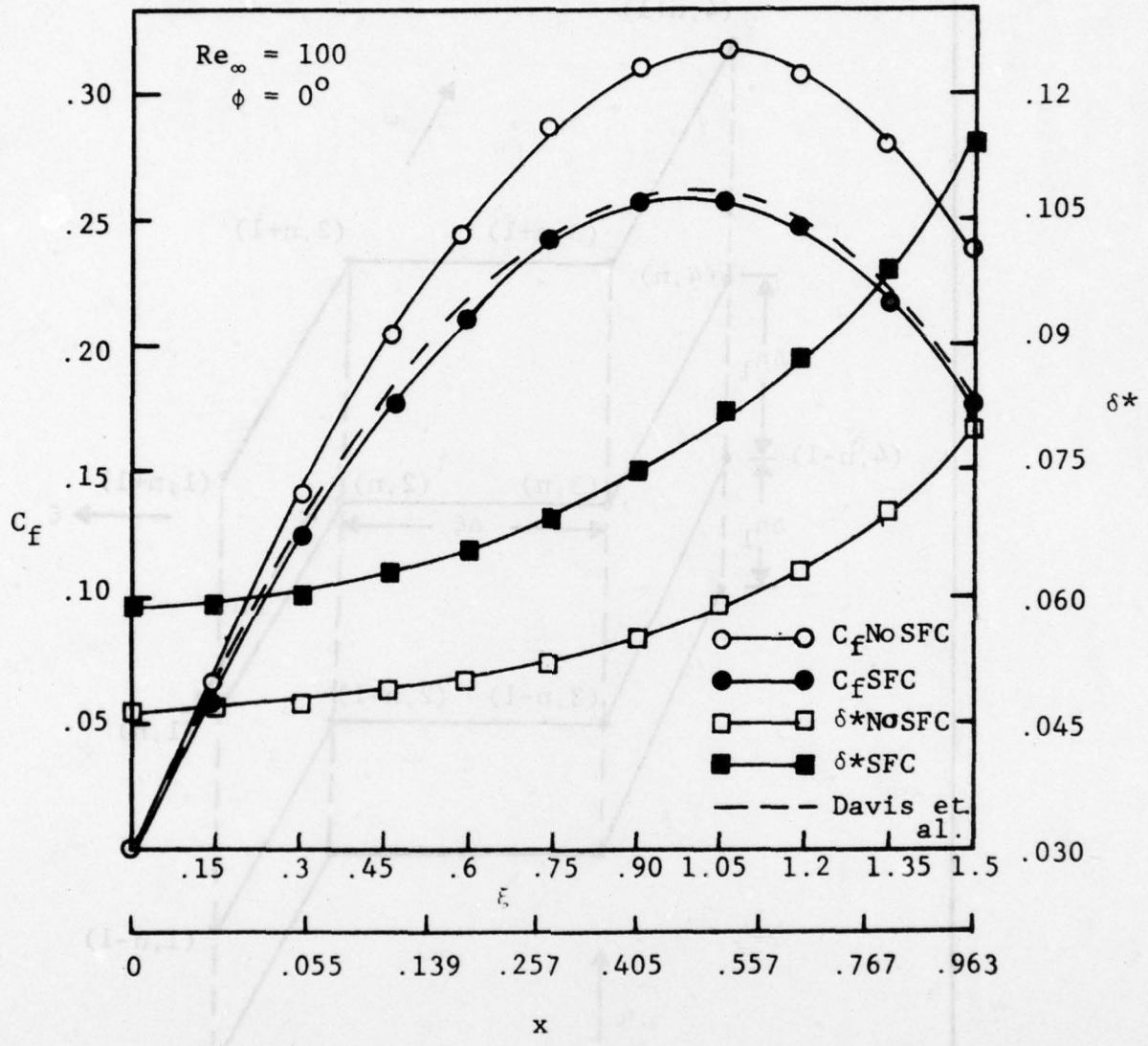

Figure 4. BOUNDARY-LAYER DEVELOPMENT ALONG WINDWARD STREAMLINE OF A SPHERE AT $\alpha = 2^{o}$

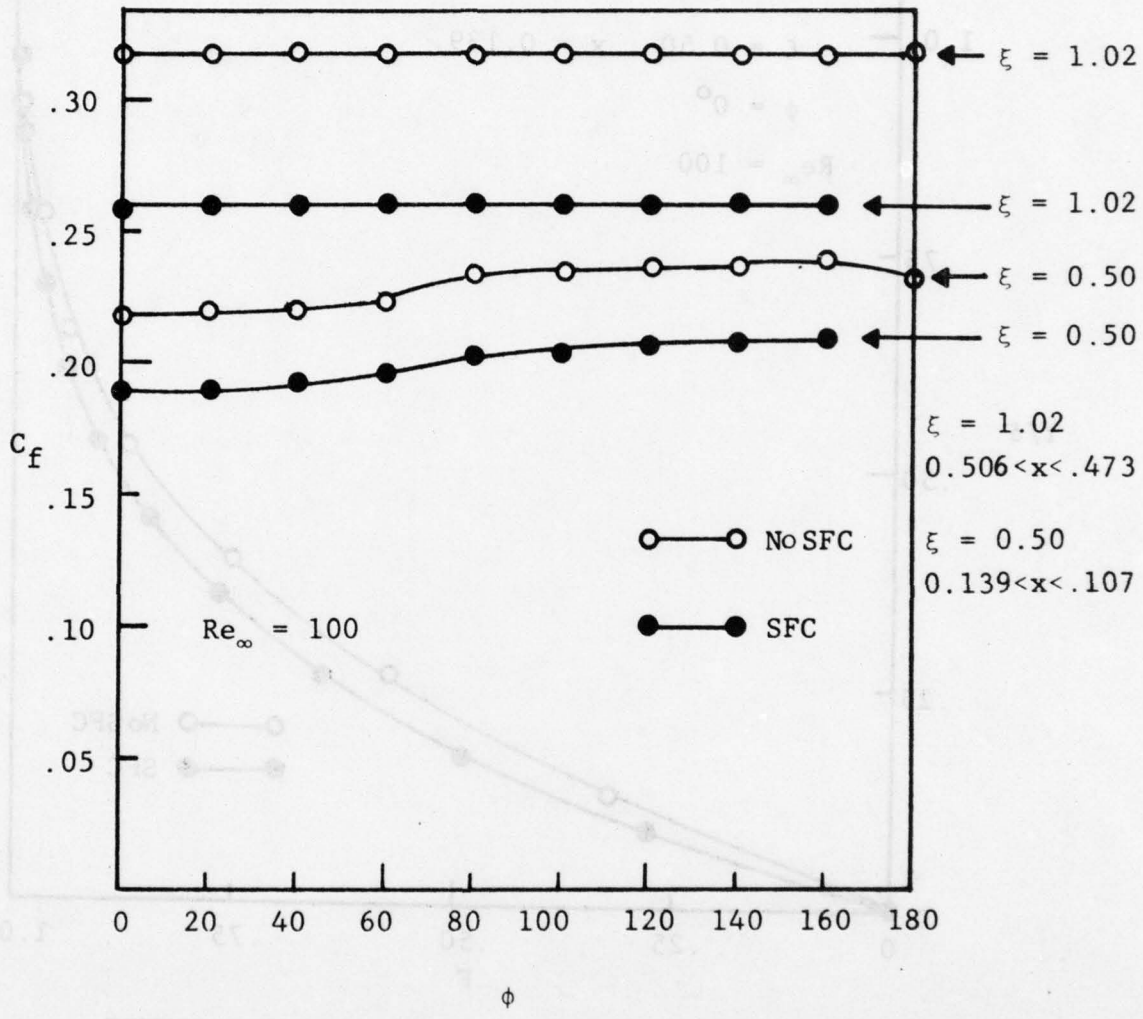

Figure 5. SKIN FRICTION DISTRIBUTION AROUND A SPHERE AT $\alpha = 2^o$

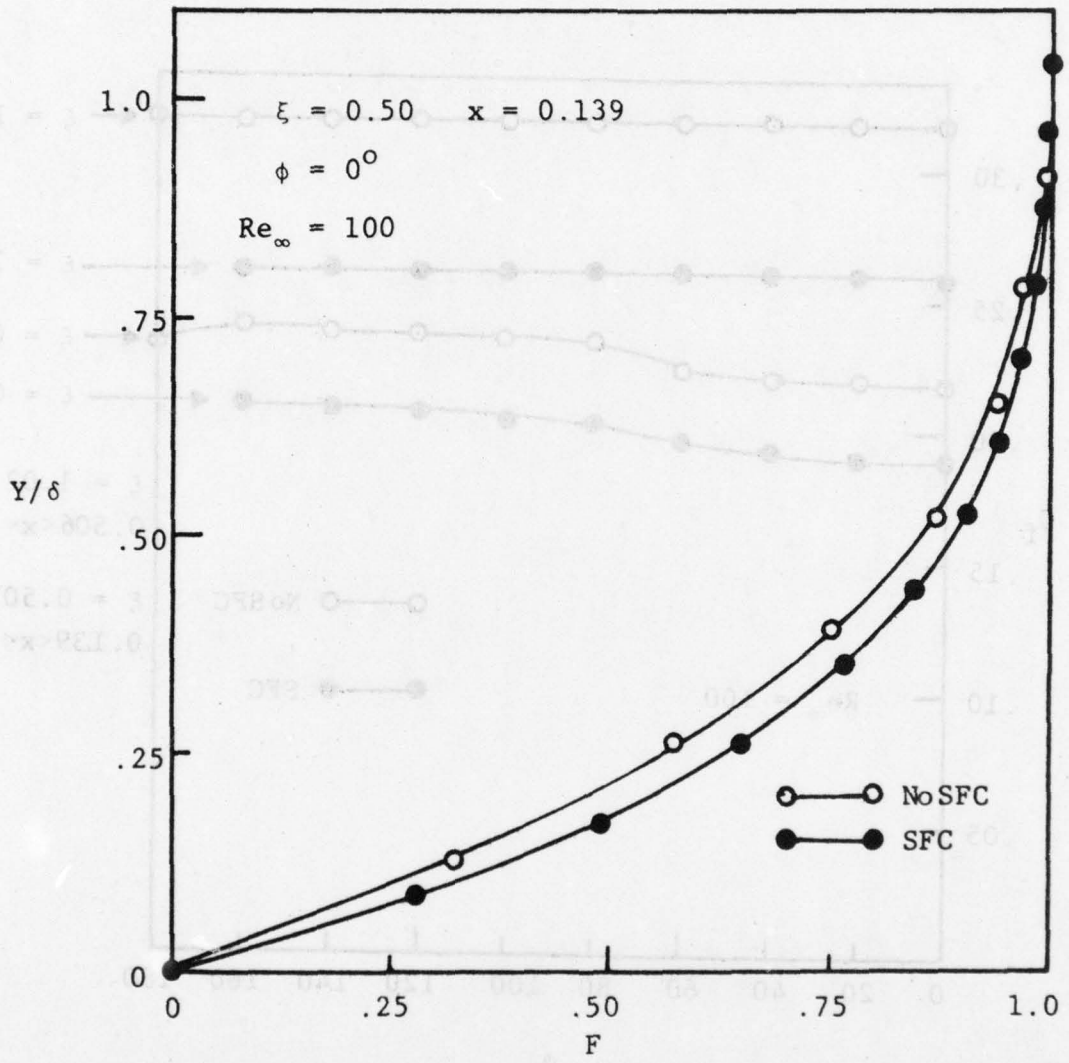

Figure 6. BOUNDARY-LAYER PROFILES FOR SPHERE, $\alpha = 2^{o}$

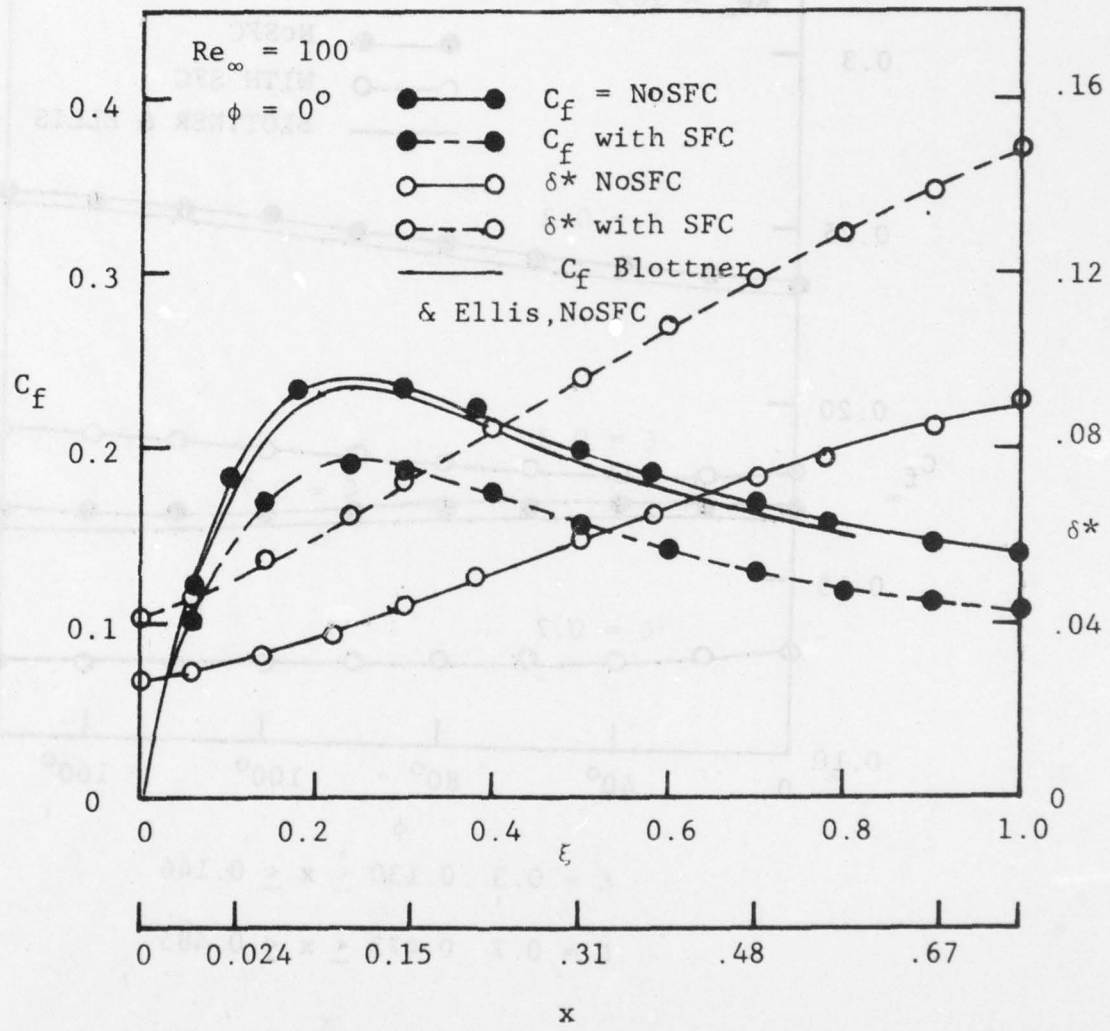

Figure 7. BOUNDARY-LAYER DEVELOPMENT ALONG WINDWARD STREAMLINE OF A 4:1 SPHEROID at $\alpha = 2^{o}$

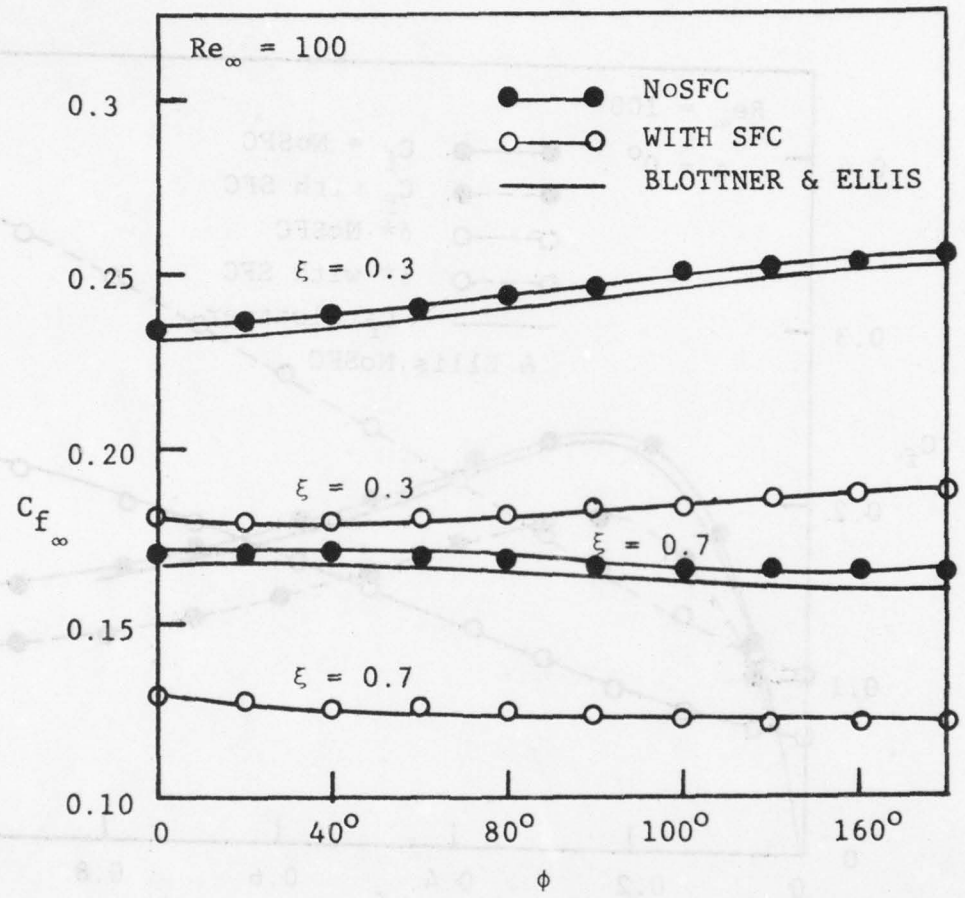

$\xi = 0.3 \quad 0.130 \leq x \leq 0.146$

$\xi = 0.7 \quad 0.473 \leq x \leq 0.485$

Figure 8. SKIN FRICTION AROUND A 4:1 SPHEROID AT $\alpha = 2^{\circ}$

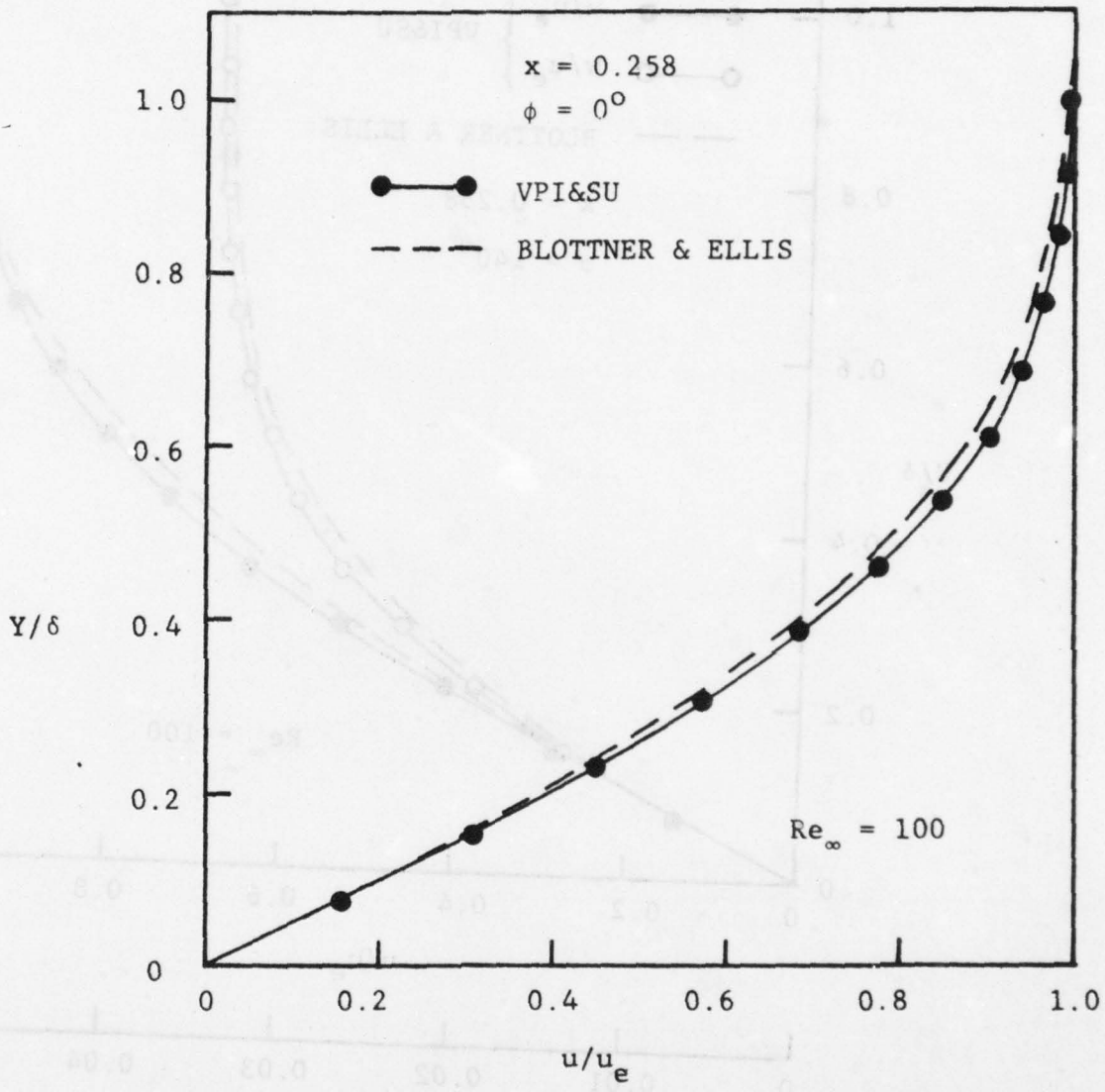

Figure 9. COMPARISON OF BOUNDARY LAYER VELOCITY PROFILE ON 4:1 SPHEROID at $\alpha = 2^o$

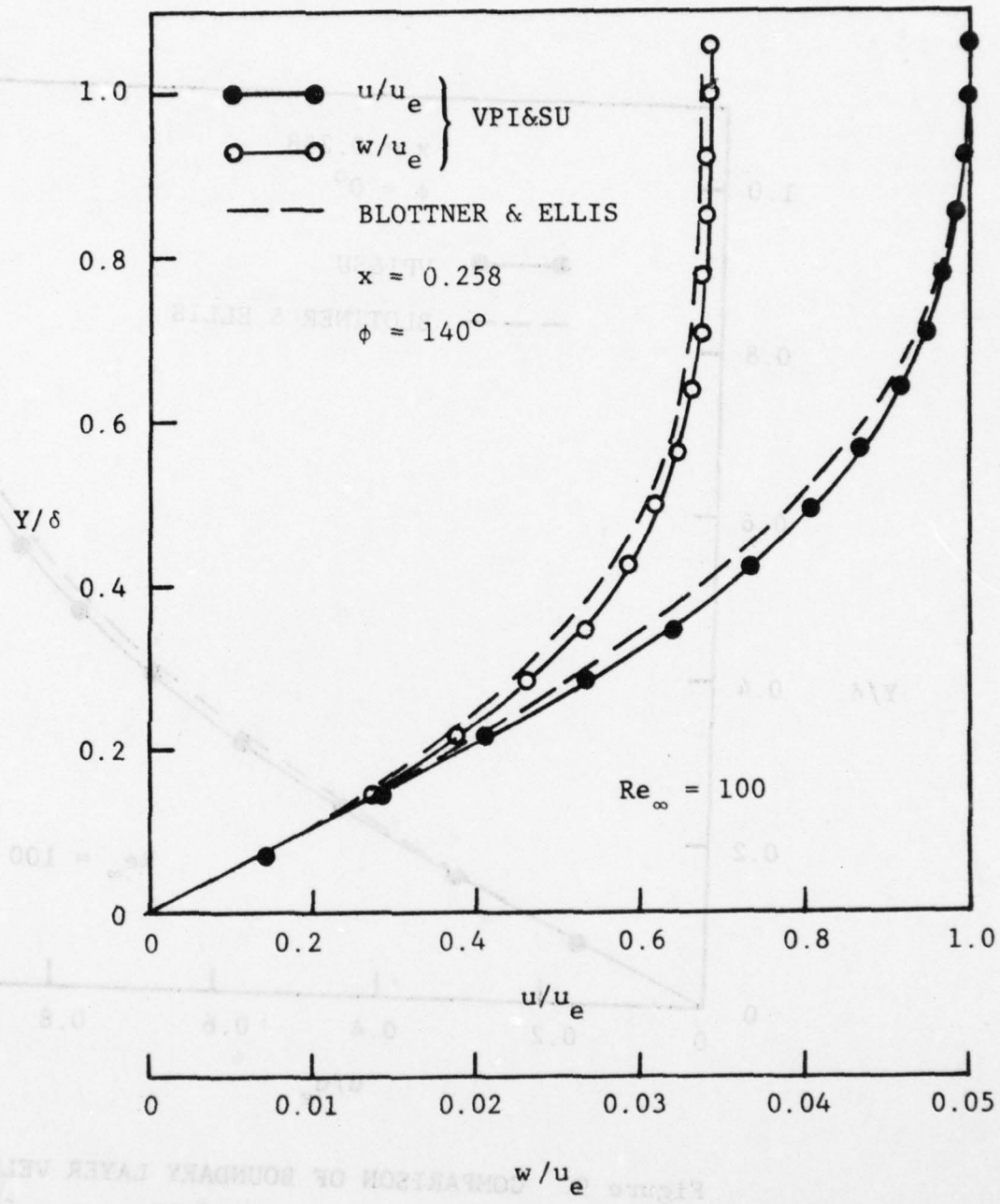

Figure 10. COMPARISON OF BOUNDARY-LAYER VELOCITY PROFILES 4:1 SPHEROID at $\alpha = 2^{\circ}$

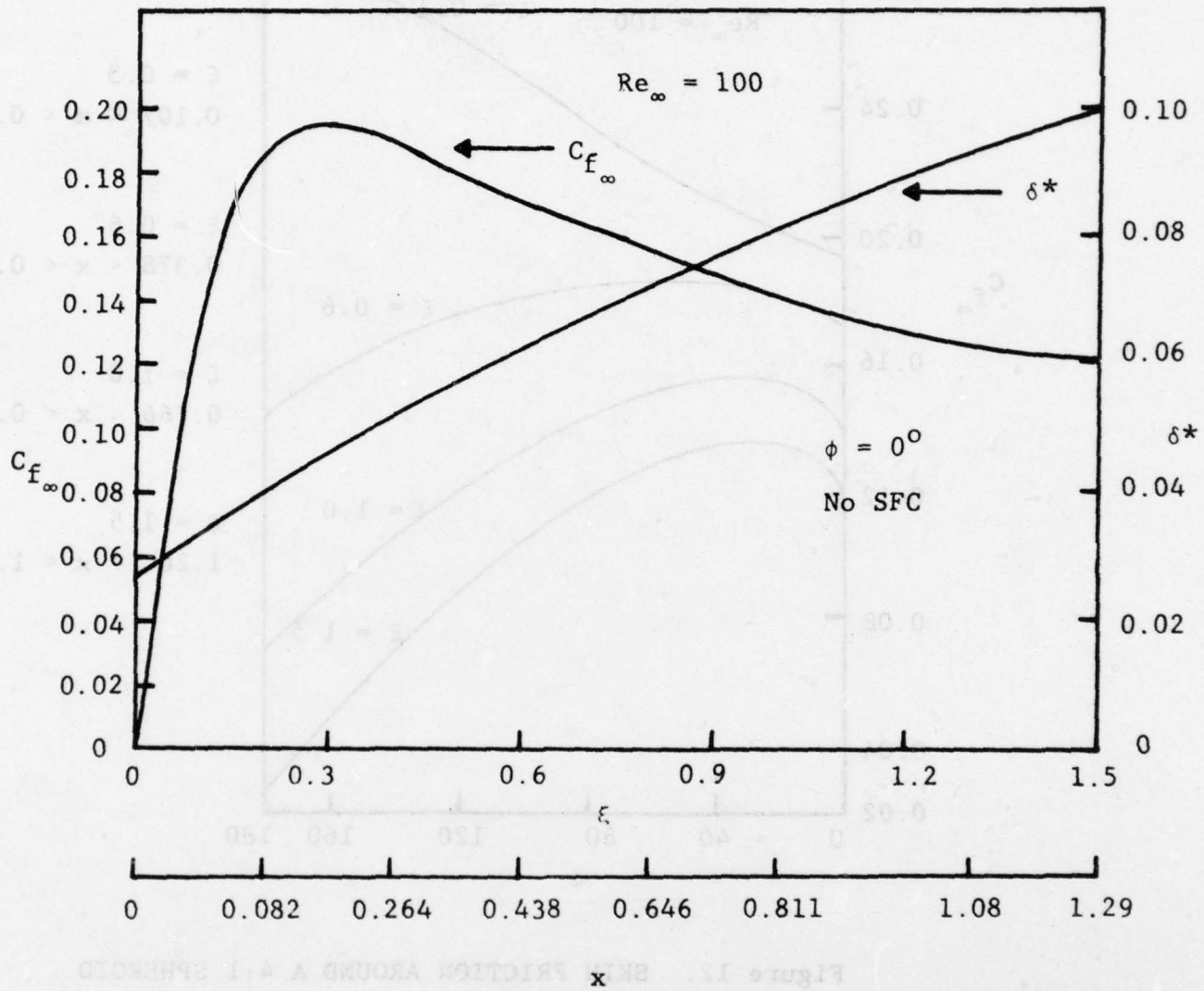

Figure 11. SKIN FRICTION ON A 4:1 SPHEROID at $\alpha = 10^{o}$

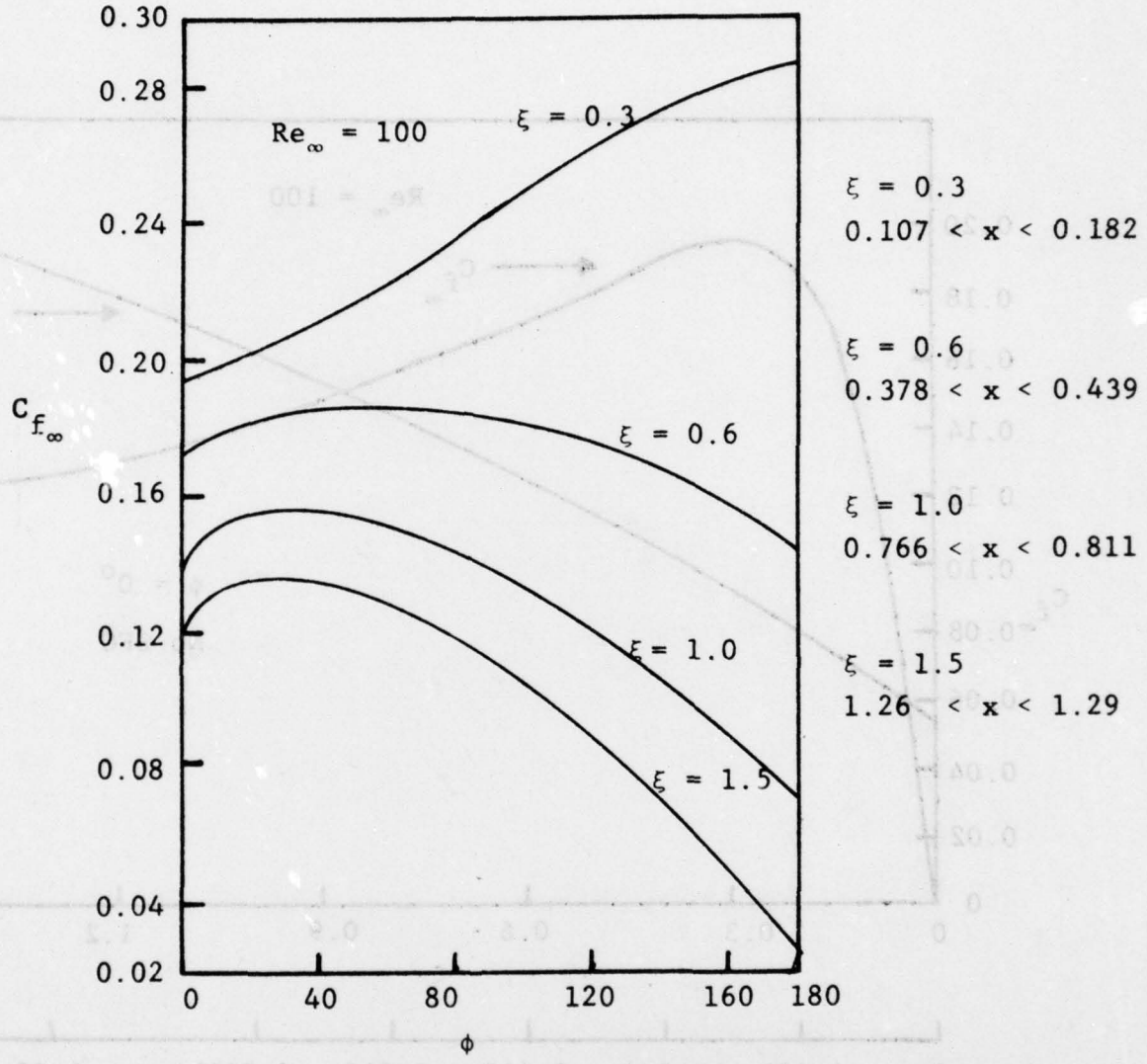

Figure 12. SKIN FRICTION AROUND A 4:1 SPHEROID at $\alpha = 10^{o}$

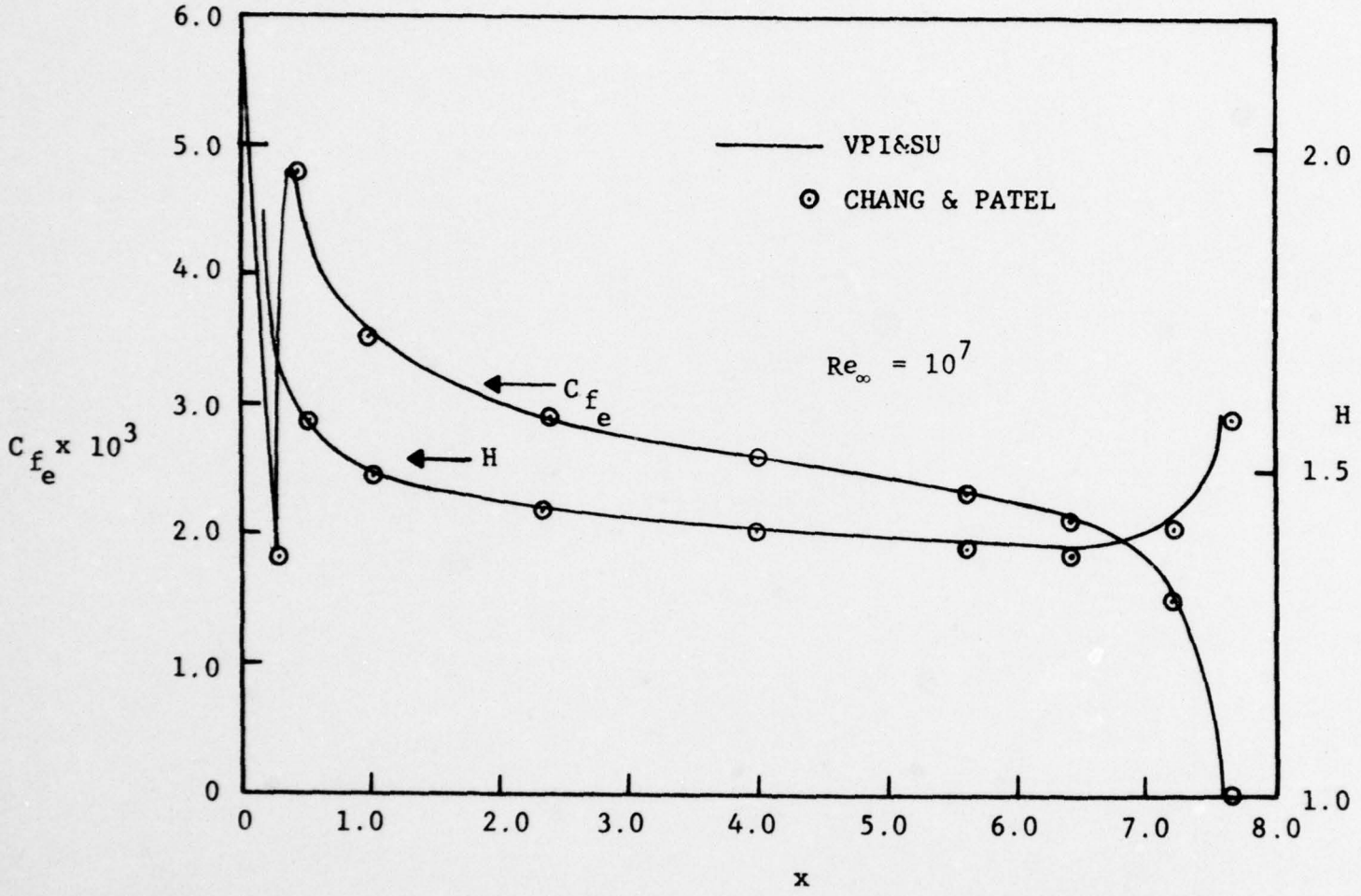

Figure 13. TURBULENT BOUNDARY-LAYER ON 4:1 SPHEROID AT ZERO ANGLE OF ATTACK